



Lifetime of the key $^{30}\text{P}(p,\gamma)^{31}\text{S}$ resonance in novae

Barry Davids, Lijie Sun, Chris Wrede

Spokespersons for S2373

TRIUMF NP-EEC Meeting, Jan 30, 2024



Bottleneck for Nova Nucleosynthesis



Presolar grains of nova origin

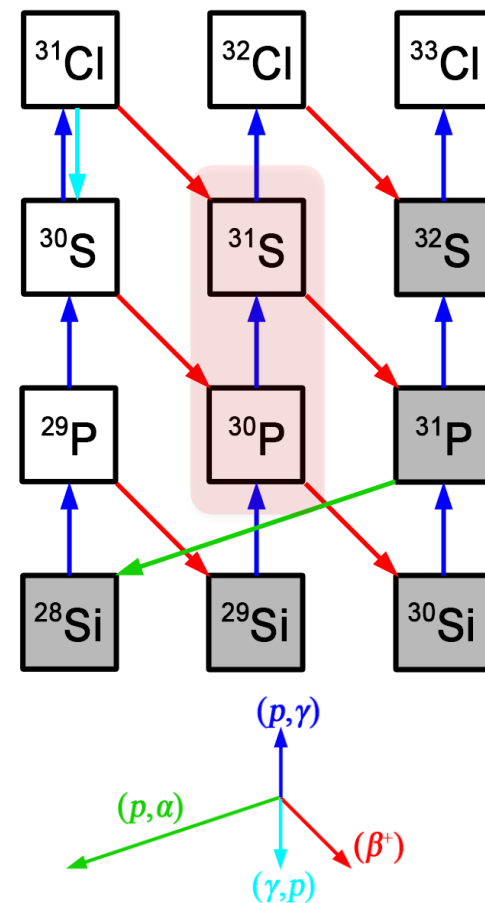
J. José *et al.*, *Astrophys. J.* 612, 414 (2004).

Nuclear thermometers for novae

L. N. Downen *et al.*, *Astrophys. J.* 762, 105 (2013).

Nuclear mixing meters for novae

K. J. Kelly *et al.*, *Astrophys. J.* 777, 130 (2013).



J. José *et al.*, *Nucl. Phys. A* 777, 550 (2006).
 C. Wrede, *AIP Advances* 4, 041004 (2014).

Thermonuclear $^{30}\text{P}(p,\gamma)^{31}\text{S}$ Reaction Rate

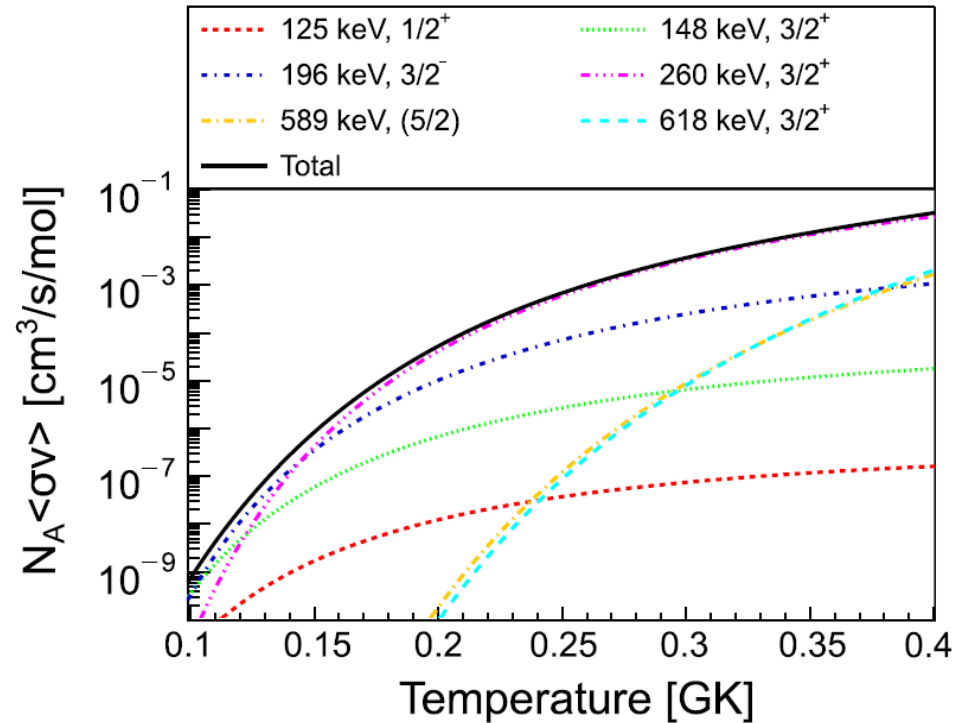
Resonant reaction rate

$$N_A \langle \sigma v \rangle_{\text{res}} = N_A \left(\frac{2\pi}{\mu kT} \right)^{3/2} \hbar^2 \omega \gamma \exp\left(-\frac{E_r}{kT}\right)$$

Resonance strength

$$\omega \gamma = \frac{2J_r + 1}{(2J_p + 1)(2J_T + 1)} \frac{\Gamma_p \Gamma_\gamma}{\Gamma} \quad \Gamma = \frac{\hbar}{\tau}$$

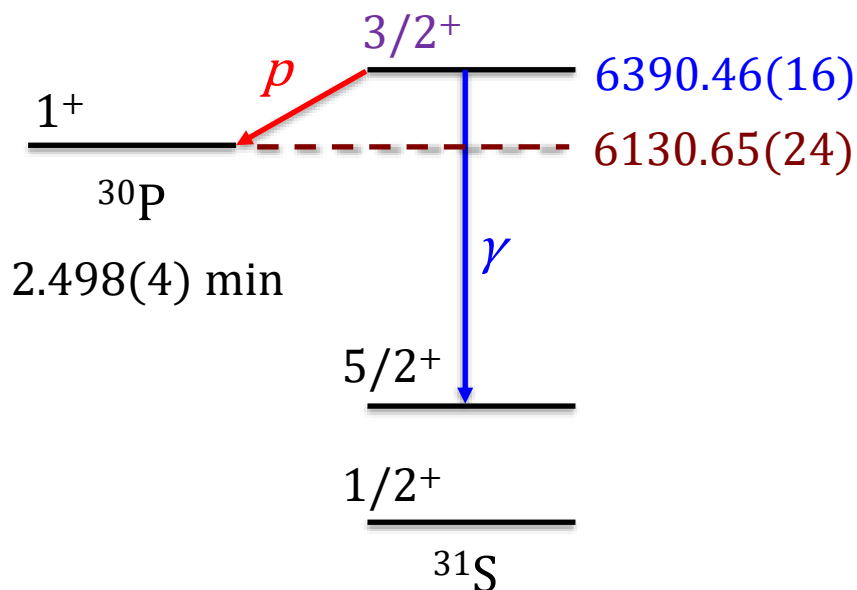
$$= \frac{2J_r + 1}{(2J_p + 1)(2J_T + 1)} B_p (1 - B_p) \frac{\hbar}{\tau}$$



T. Budner *et al.*, Phys. Rev. Lett. 128, 182701 (2022).

C. Iliadis, Nuclear Physics of Stars, Wiley-VCH, 2015.

Key $^{30}\text{P}(p,\gamma)^{31}\text{S}$ Resonance



$$J^\pi = 3/2^+, E_x = 6390.2(7) \text{ keV}$$

M. B. Bennett *et al.*, Phys. Rev. Lett. 116, 102502 (2016).

$$B_p = 2.5_{-0.3}^{+0.4} \times 10^{-4}$$

T. Budner *et al.*, Phys. Rev. Lett. 128, 182701 (2022).

$$\tau = 4.4 \text{ fs (USDA)}$$

$$\tau = 26 \text{ fs (USDB)}$$

$$\tau = 3.4 \text{ fs (USDC), 1.3 fs (USDC-shifted)}$$

$$\tau = 1.9 \text{ fs (USDE)}$$

$$\tau = 3.5 \text{ fs (USDI)}$$

B. A. Brown. Shell Model Calculations.

$$\tau < 10 \text{ fs } (^{31}\text{P } 3/2^+ 6381 \text{ keV})$$

E.O. de Neijs *et al.*, Nucl. Phys. A 254, 45 (1975).

$$\tau < 20 \text{ fs (TRIUMF S1582)}$$

L. J. Sun *et al.*, Phys. Lett. B 839, 137801 (2023).

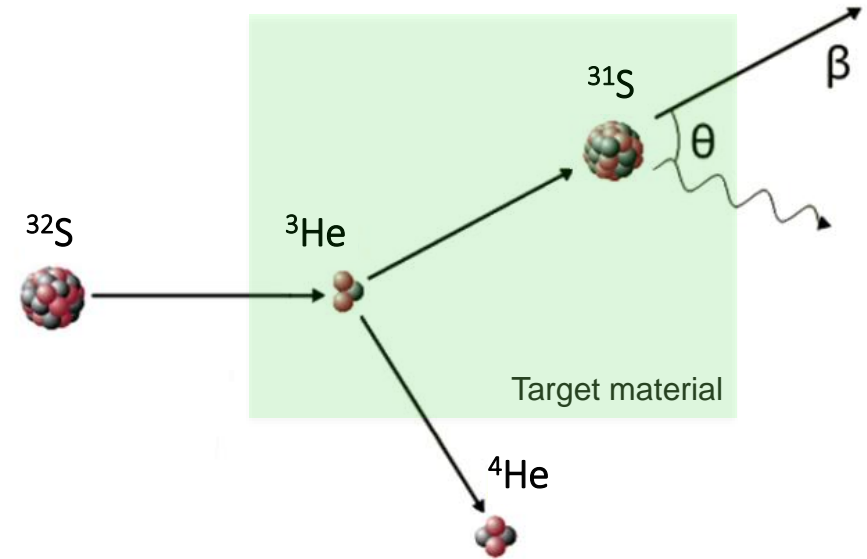
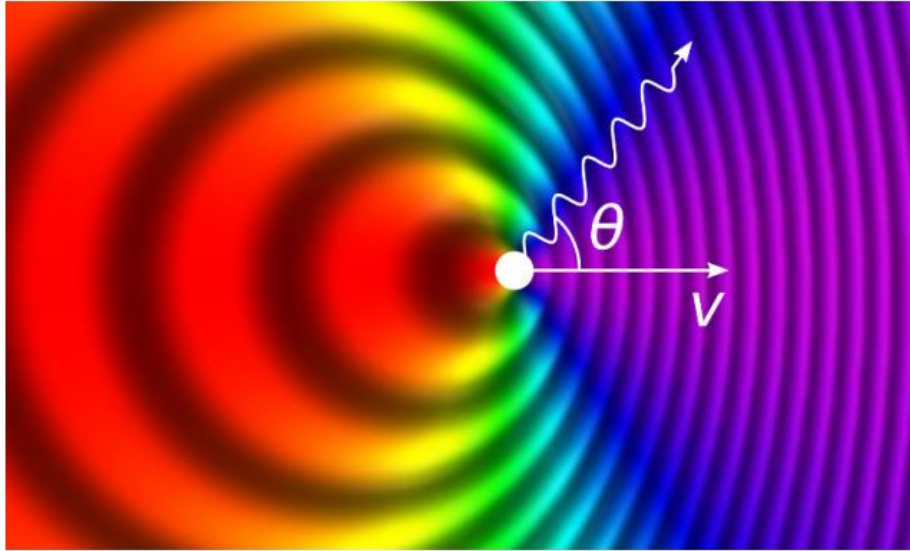
S_p :

A. Kankainen *et al.*, Phys. Rev. C 82, 052501(R) (2010).

L. Canete *et al.*, Eur. Phys. J. A 52, 124 (2016).



Doppler Shift Attenuation Method



$$E_\gamma = E_0 \frac{\sqrt{1 - \beta^2}}{1 - \beta \cos \theta}, \quad \beta = \frac{v}{c}$$

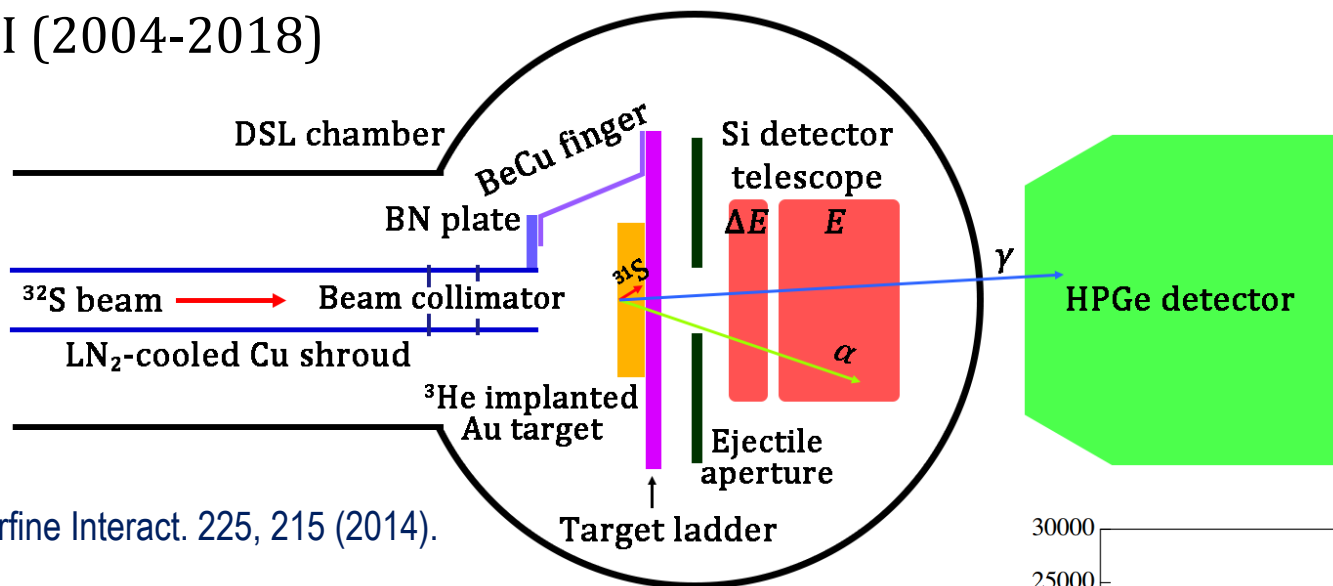
D. Branford *et al.*, Nucl. Instrum. Methods 106, 437 (1973).

T. K. Alexander *et al.*, Adv. Nucl. Phys. 10, 197 (1978).

P. J. Nolan *et al.*, Rep. Prog. Phys. 42, 1 (1979).

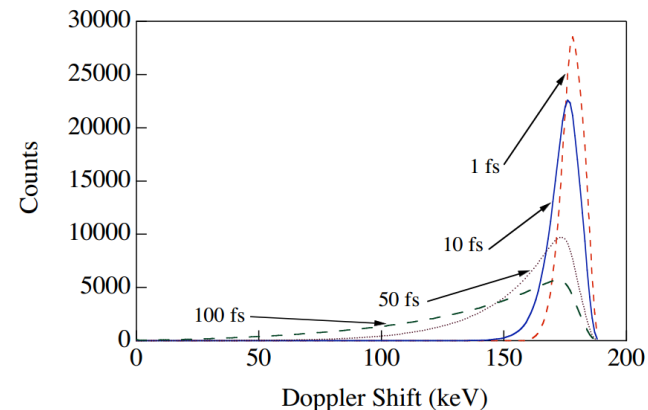
Doppler Shift Lifetimes (DSL) @ ISAC-II

DSL Phase I (2004-2018)

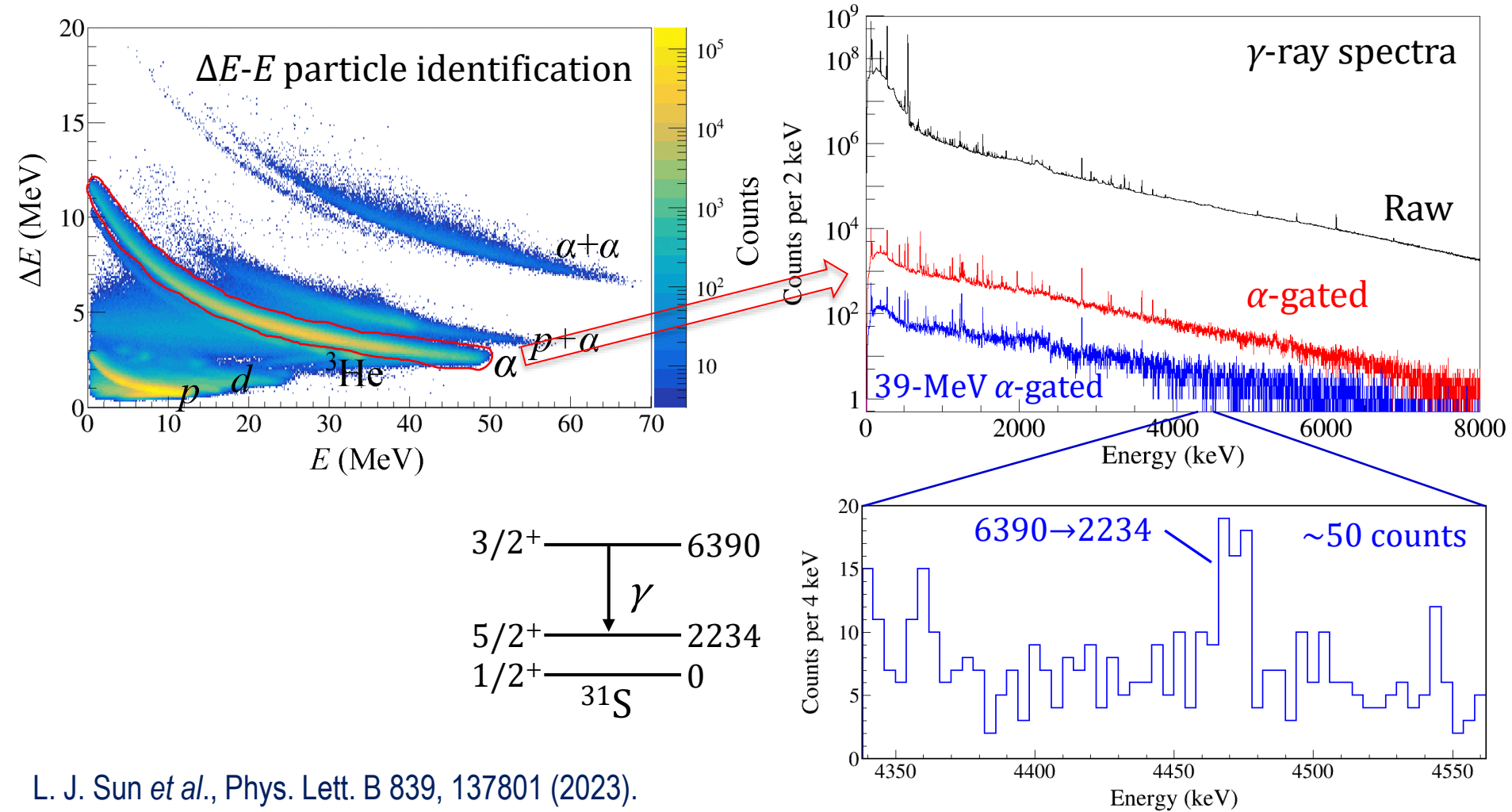


B. Davids, *Hyperfine Interact.* 225, 215 (2014).

S992	^{19}Ne	R. Kanungo <i>et al.</i> , <i>Phys. Rev. C</i> 74, 045803 (2006).
S992	^{19}Ne	S. Mythili <i>et al.</i> , <i>Phys. Rev. C</i> 77, 035803 (2008).
S1151	^{15}O	N. Galinski <i>et al.</i> , <i>Phys. Rev. C</i> 90, 035803 (2014).
S1378	^{23}Mg	O. S. Kirsebom <i>et al.</i> , <i>Phys. Rev. C</i> 93, 025802 (2016).
S1582	^{31}S	L. J. Sun <i>et al.</i> , <i>Phys. Lett. B</i> 839, 137801 (2023).

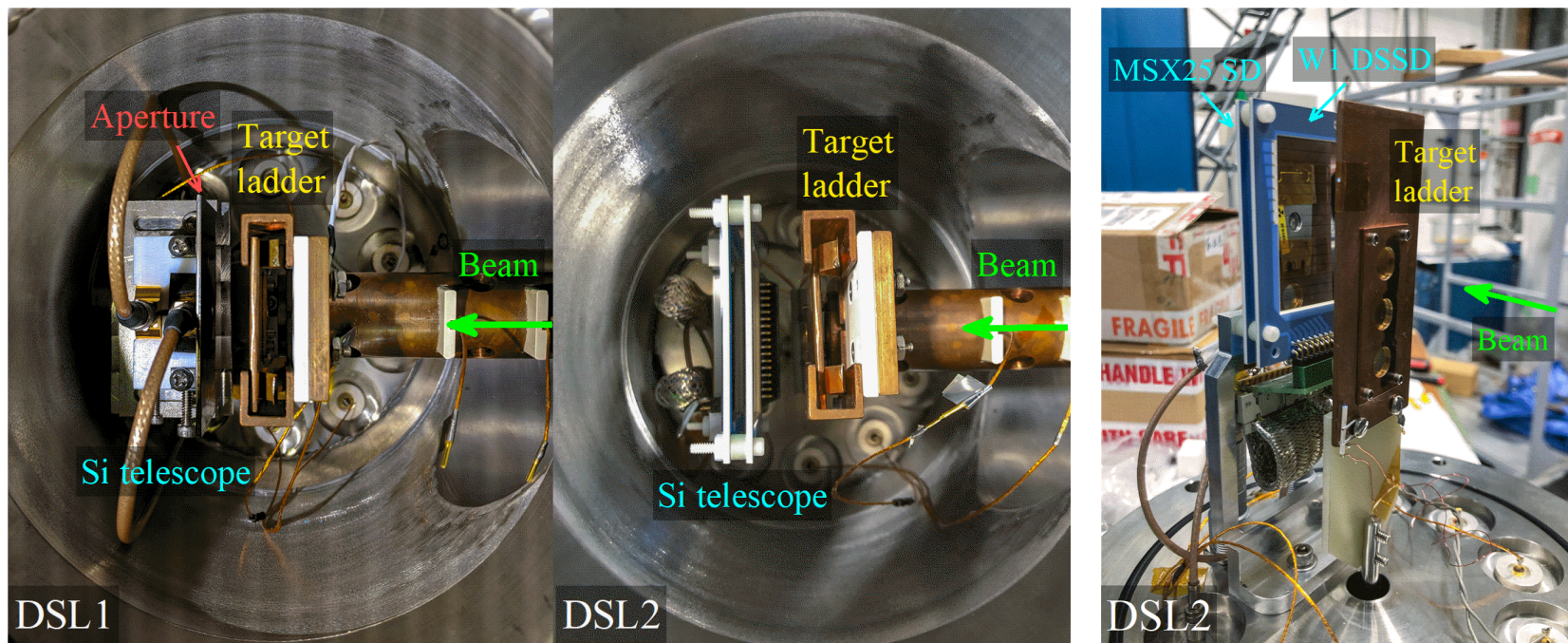


${}^3\text{He}({}^{32}\text{S}, \alpha\gamma){}^{31}\text{S}$ Reaction with DSL1



DSL2 Upgrade

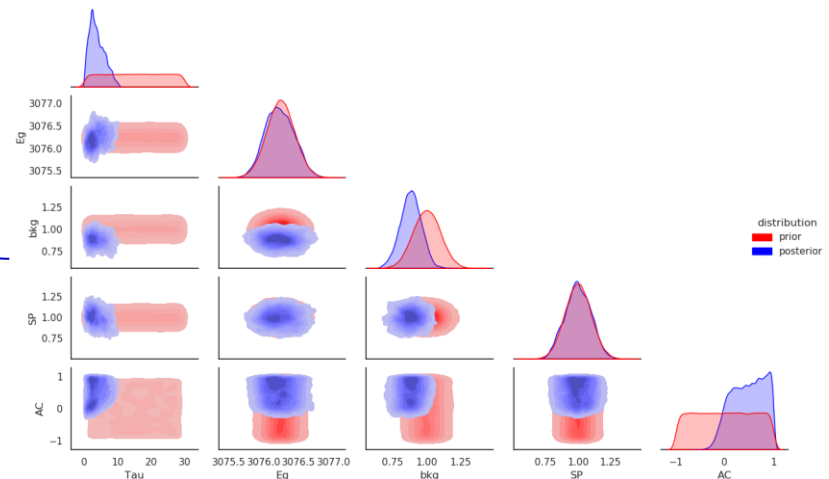
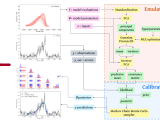
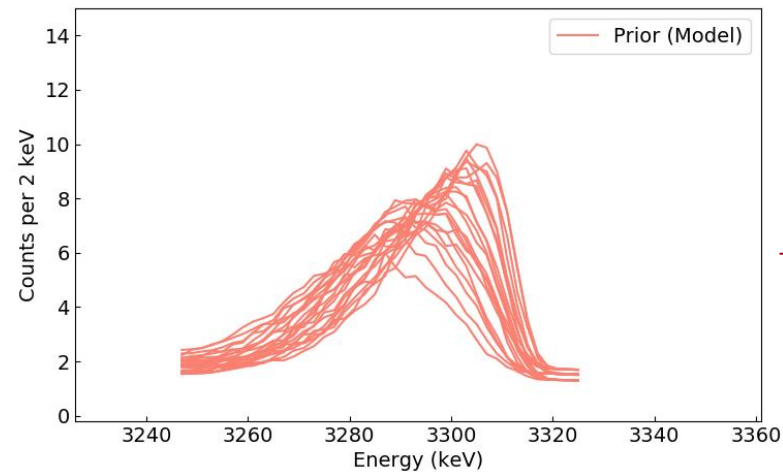
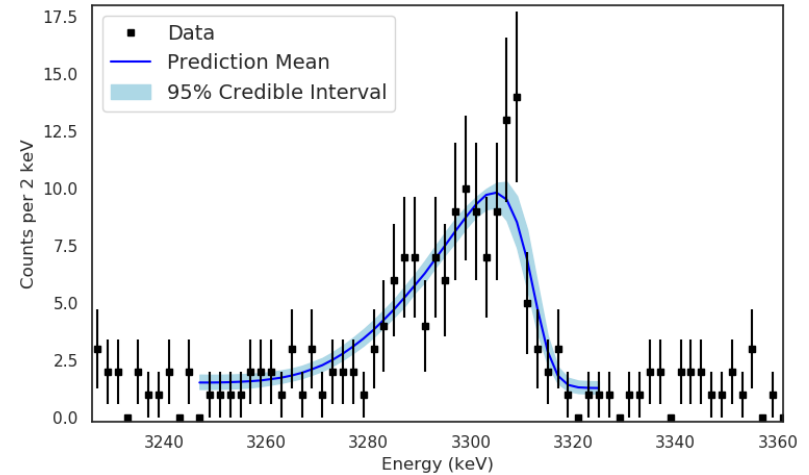
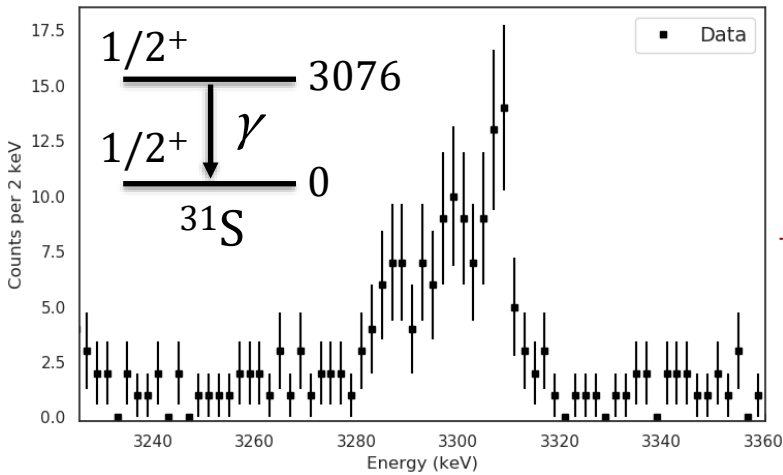
DSL Phase II (2020-)



α detection efficiency $\times 11$
 γ detection efficiency $\times 1.3$
 ~ 1000 counts with 19 shifts

S2193	^{23}Mg	L. E. Weghorn, PhD Thesis Project.
S2373	^{31}S	Proposed to NP-EEC 202401

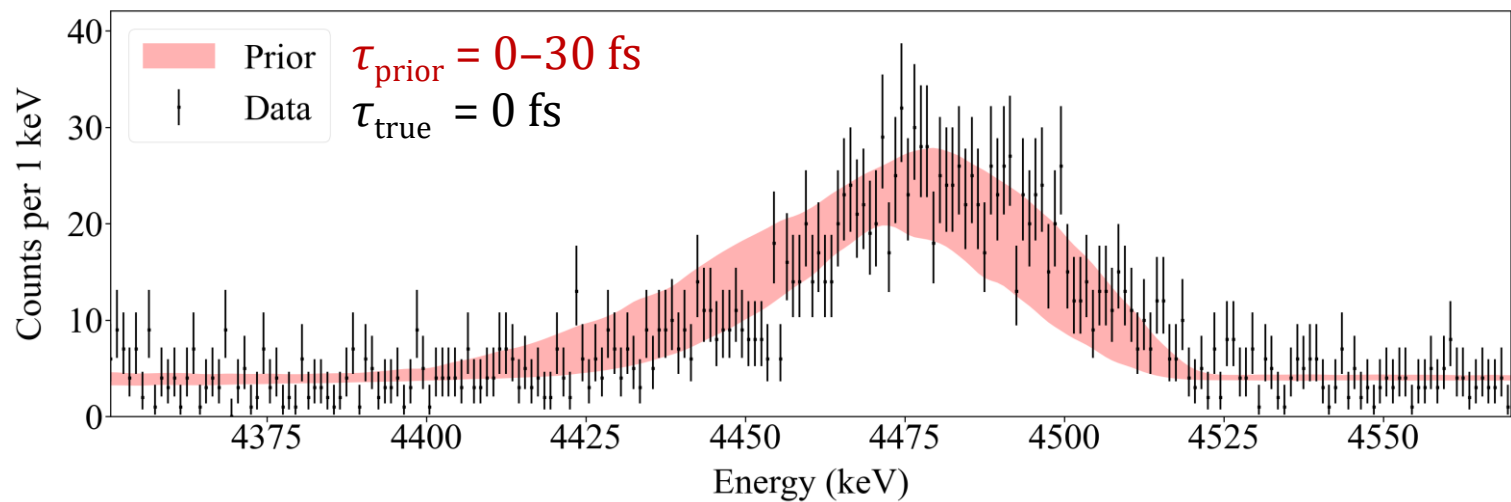
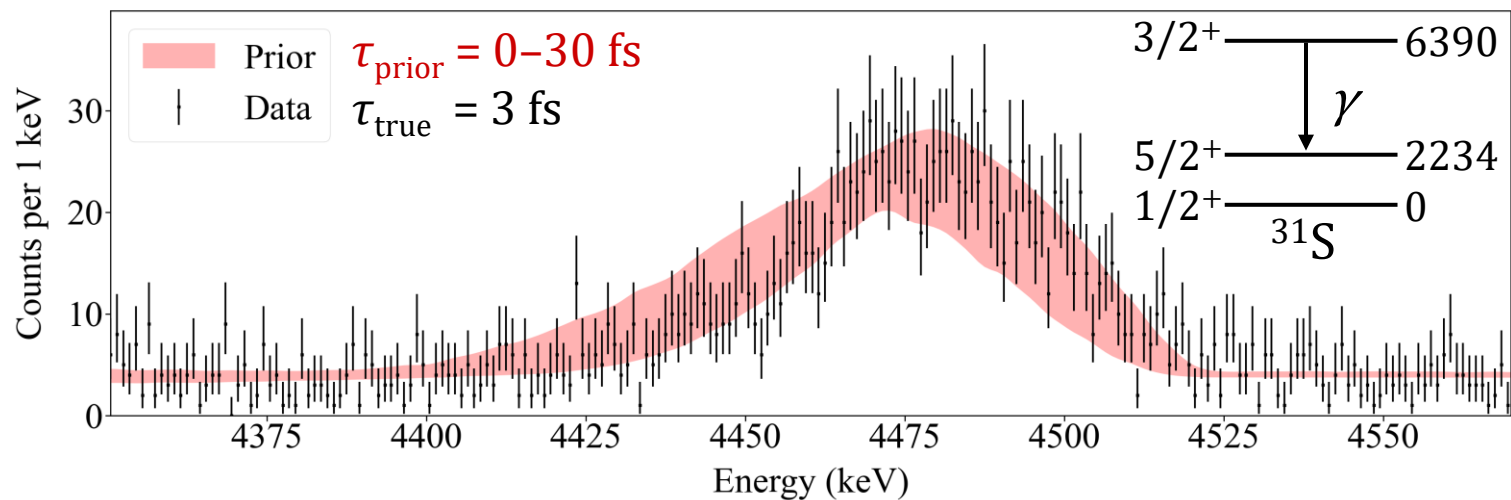
Bayesian Uncertainty Quantification



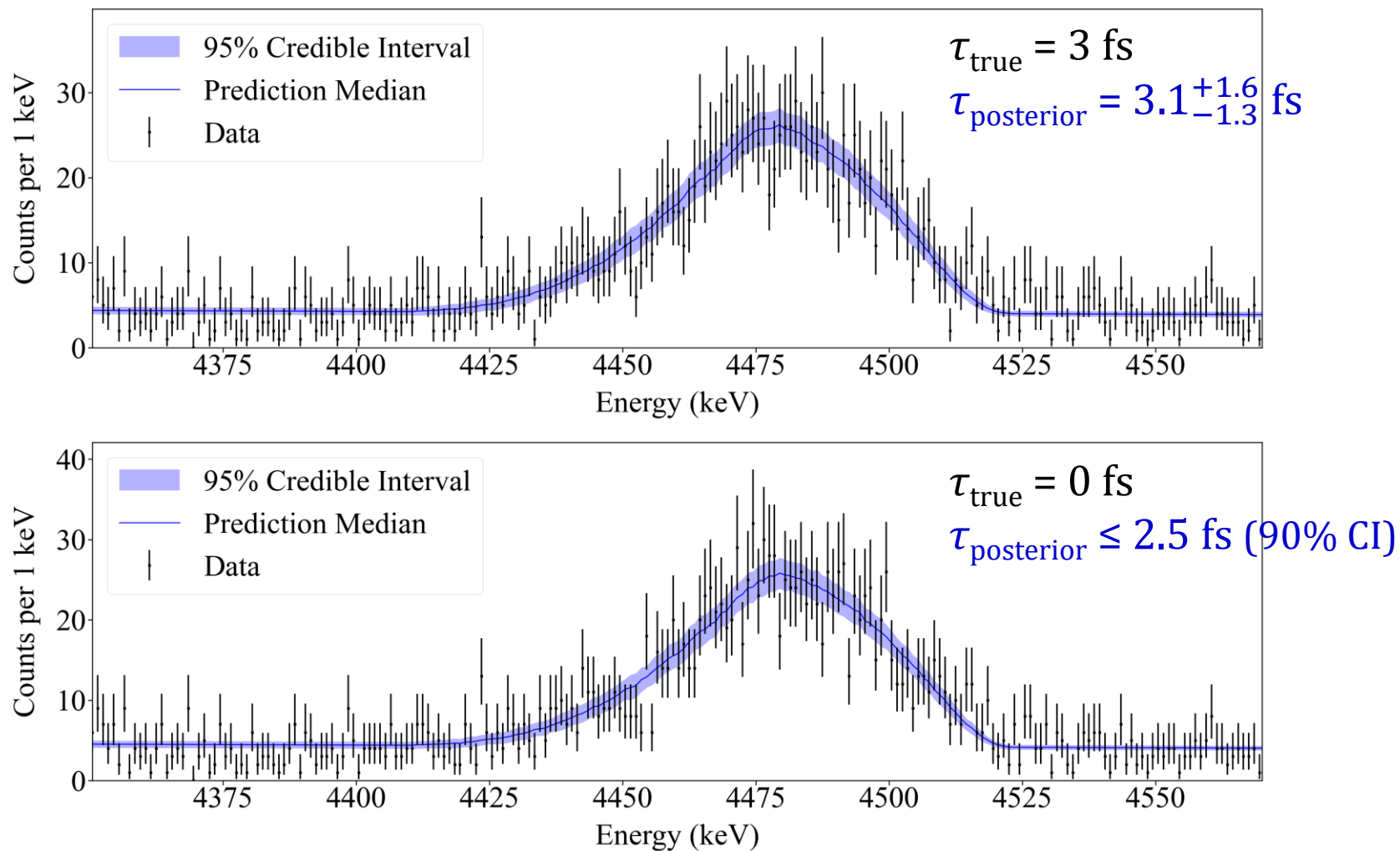
S1582 L. J. Sun *et al.*, Phys. Lett. B 839, 137801 (2023).

Ö. Sürer *et al.*, Phys. Rev. C 106, 024607 (2022).

Prior Lineshape

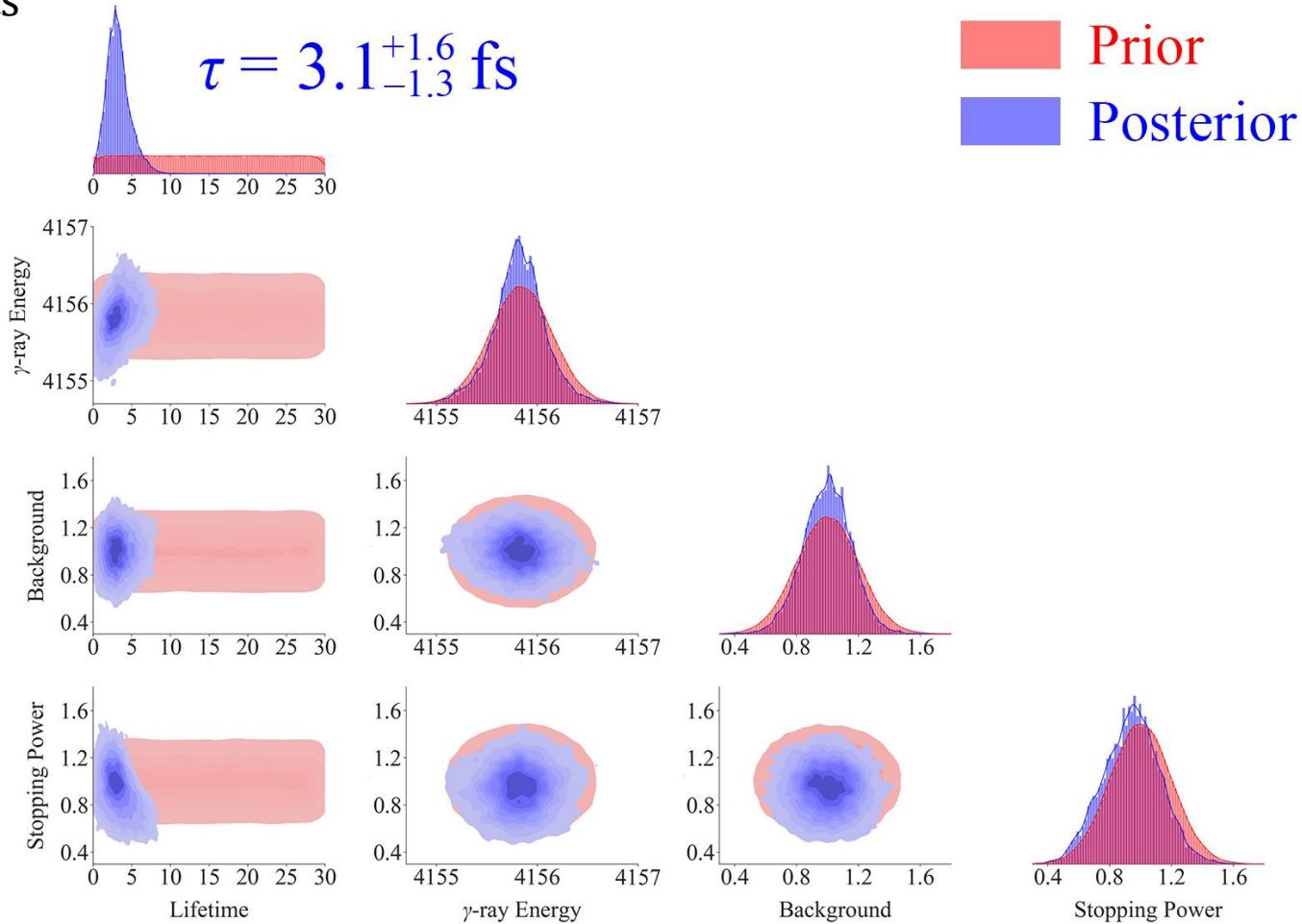


Posterior Predictive Lineshape



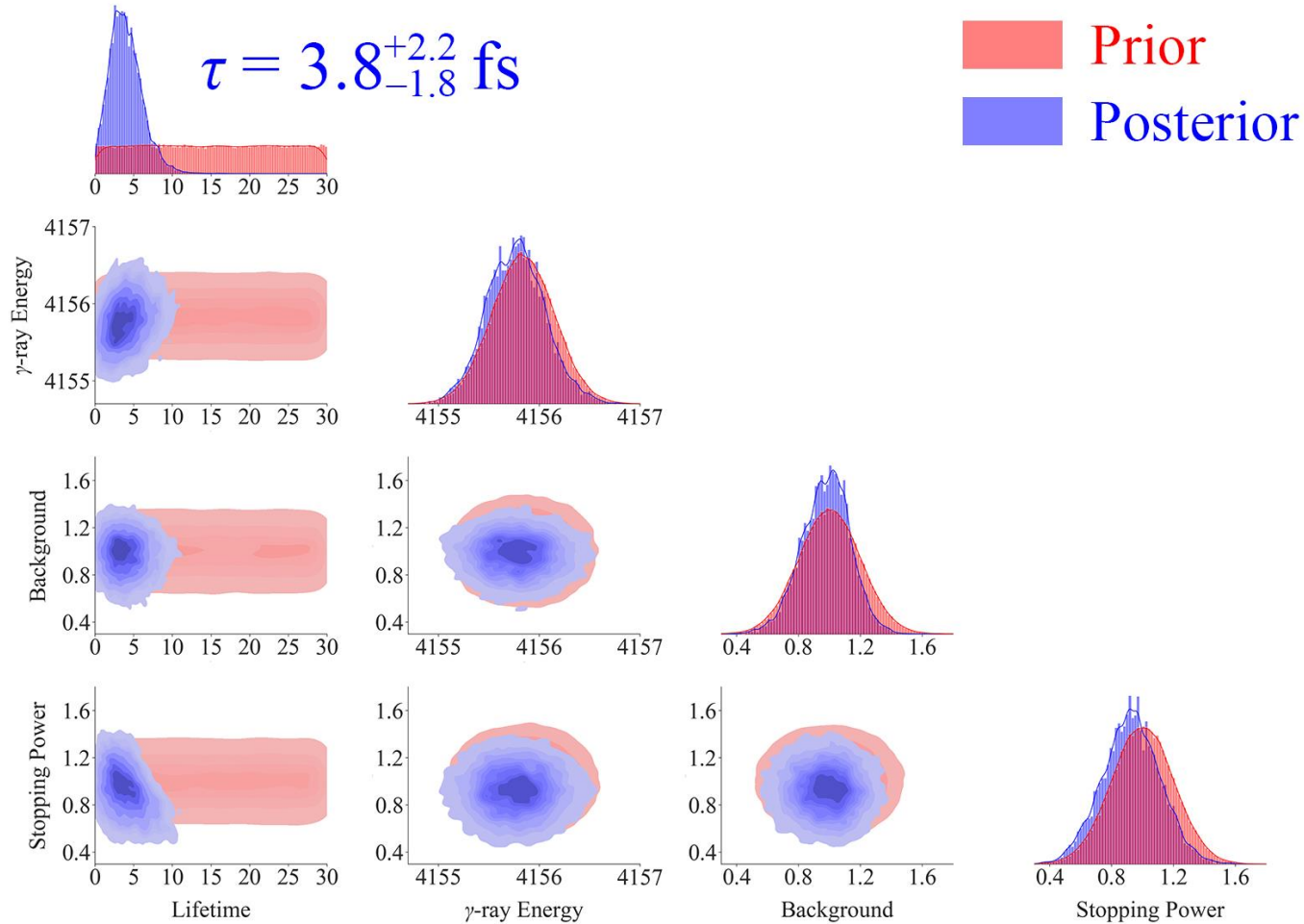
Posterior Distribution of Model Parameters

1000 counts



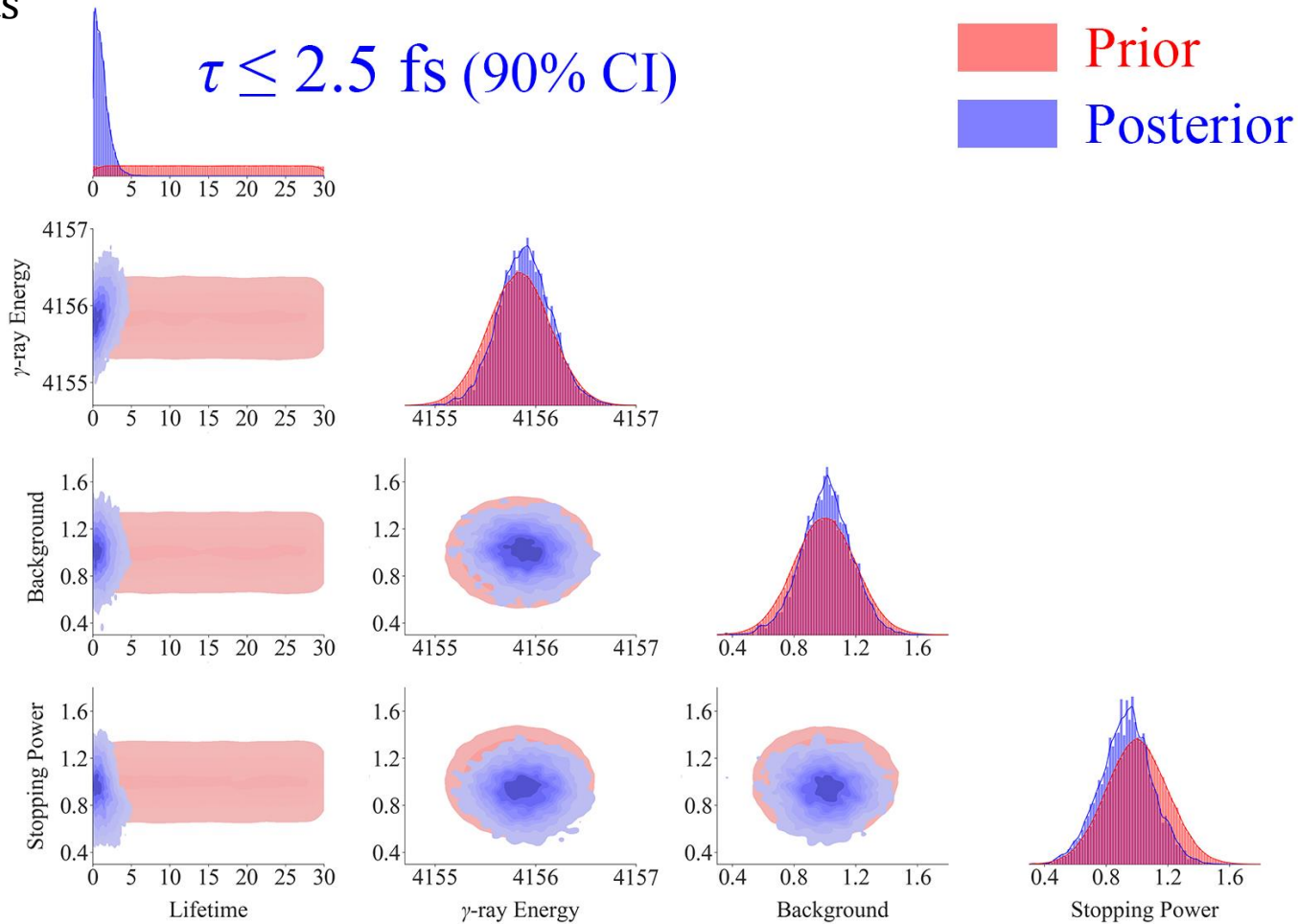
Posterior Distribution of Model Parameters

500 counts



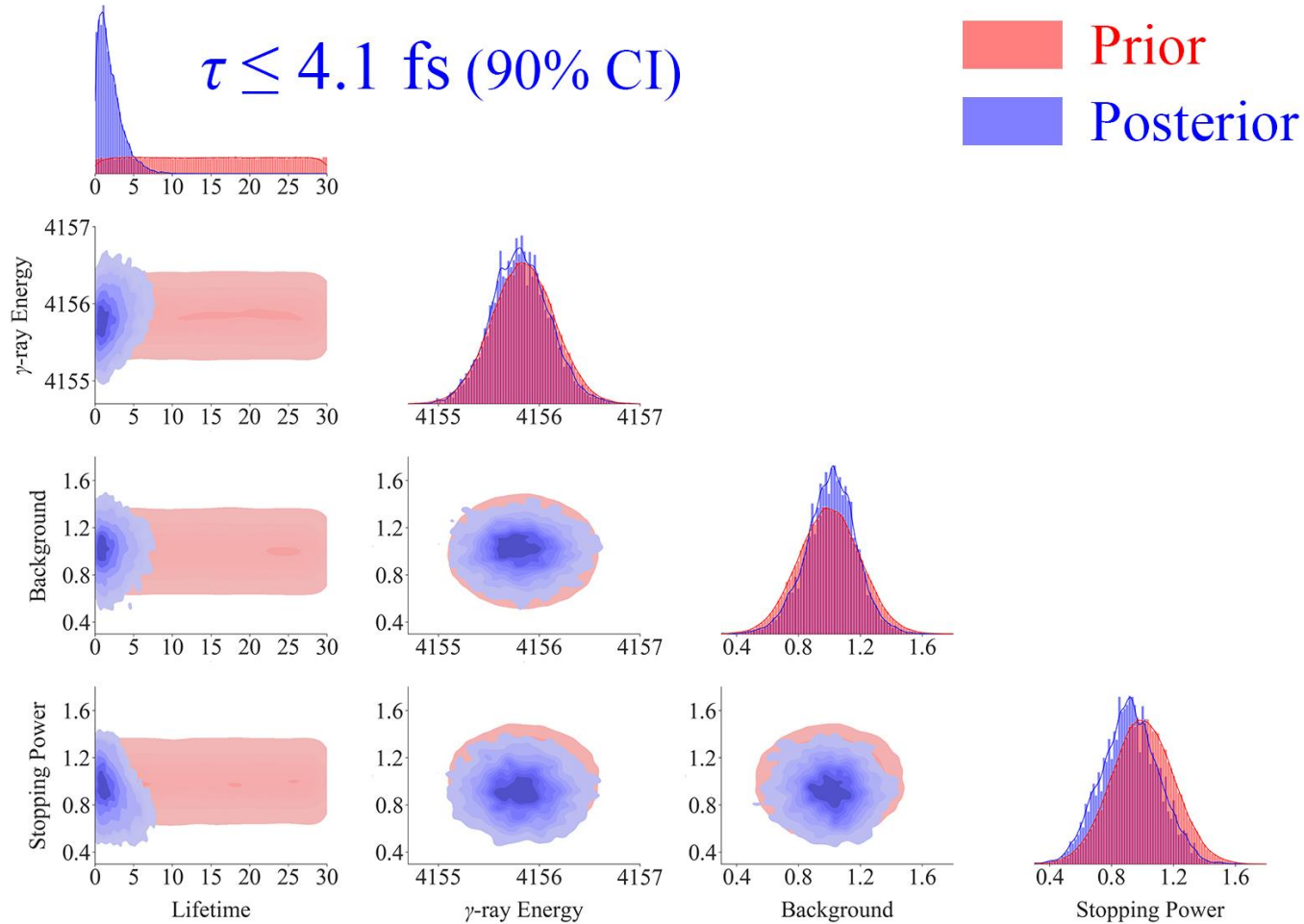
Posterior Distribution of Model Parameters

1000 counts



Posterior Distribution of Model Parameters

500 counts

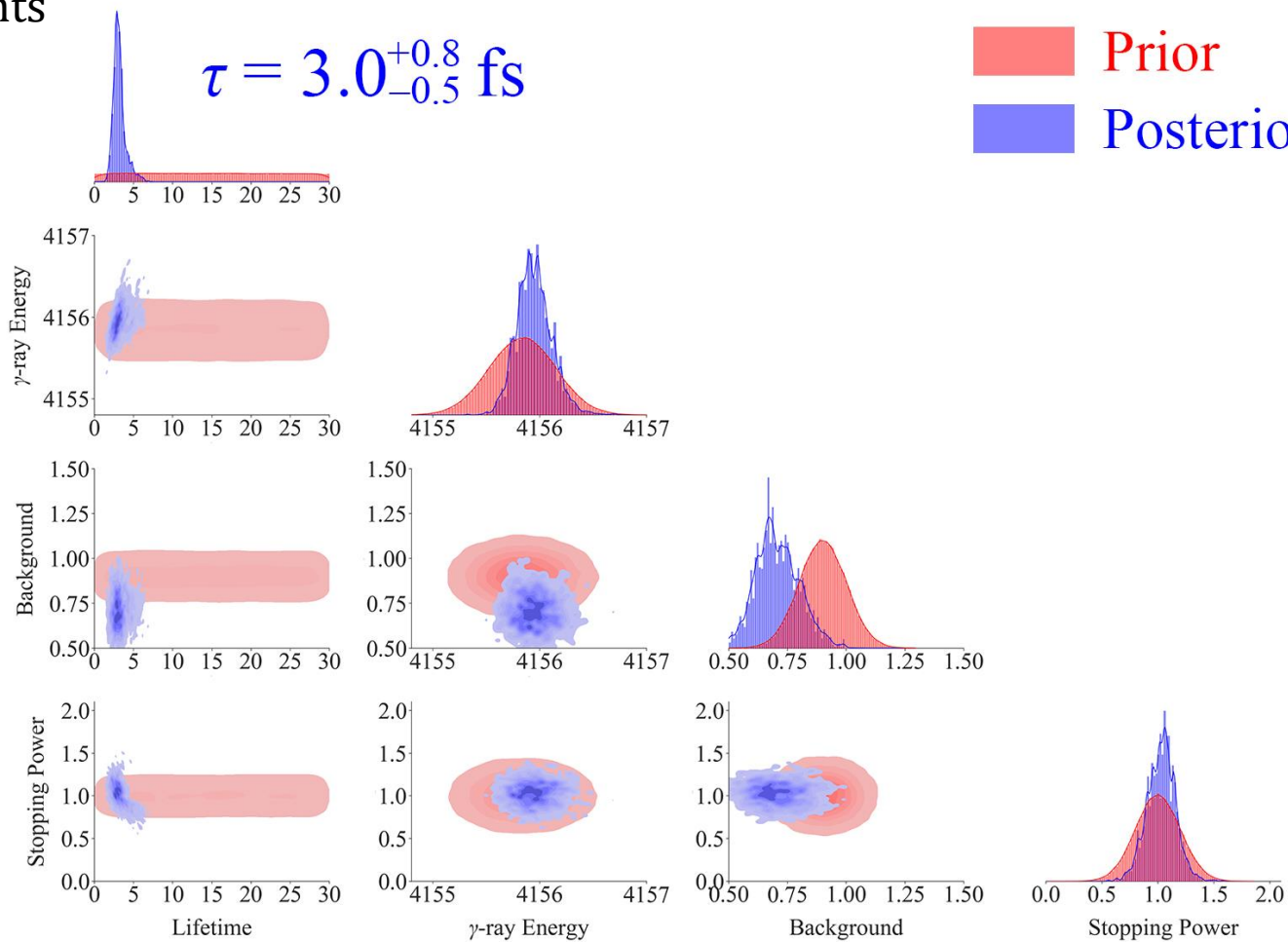


Posterior Distribution of Model Parameters

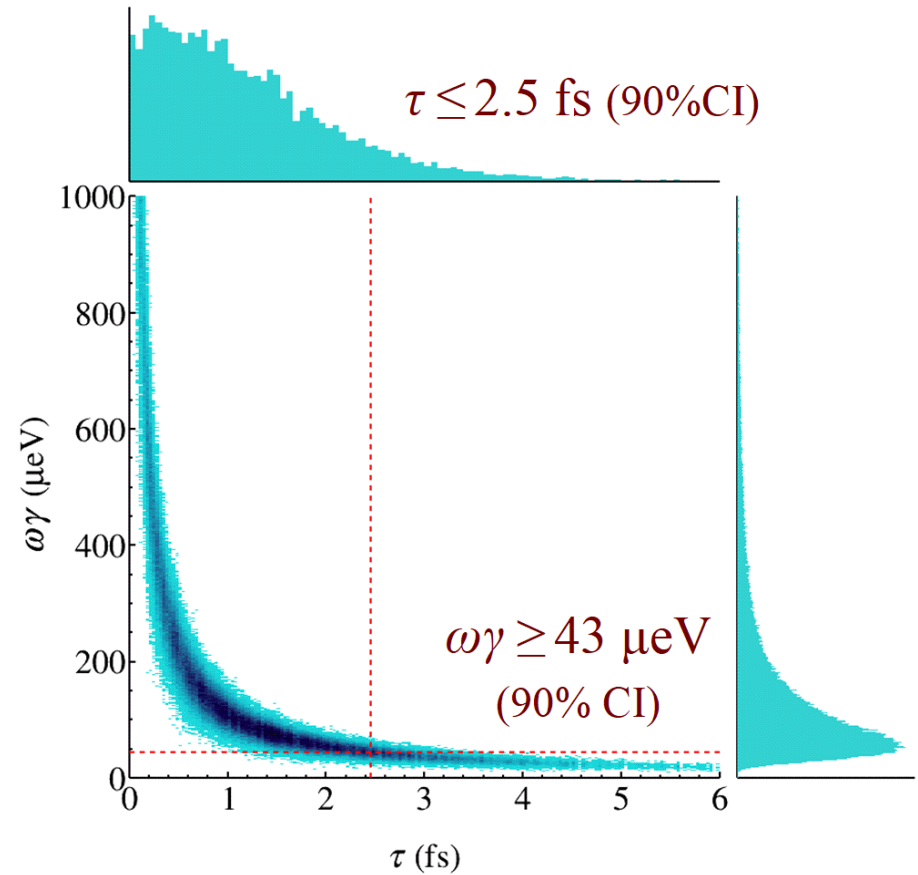
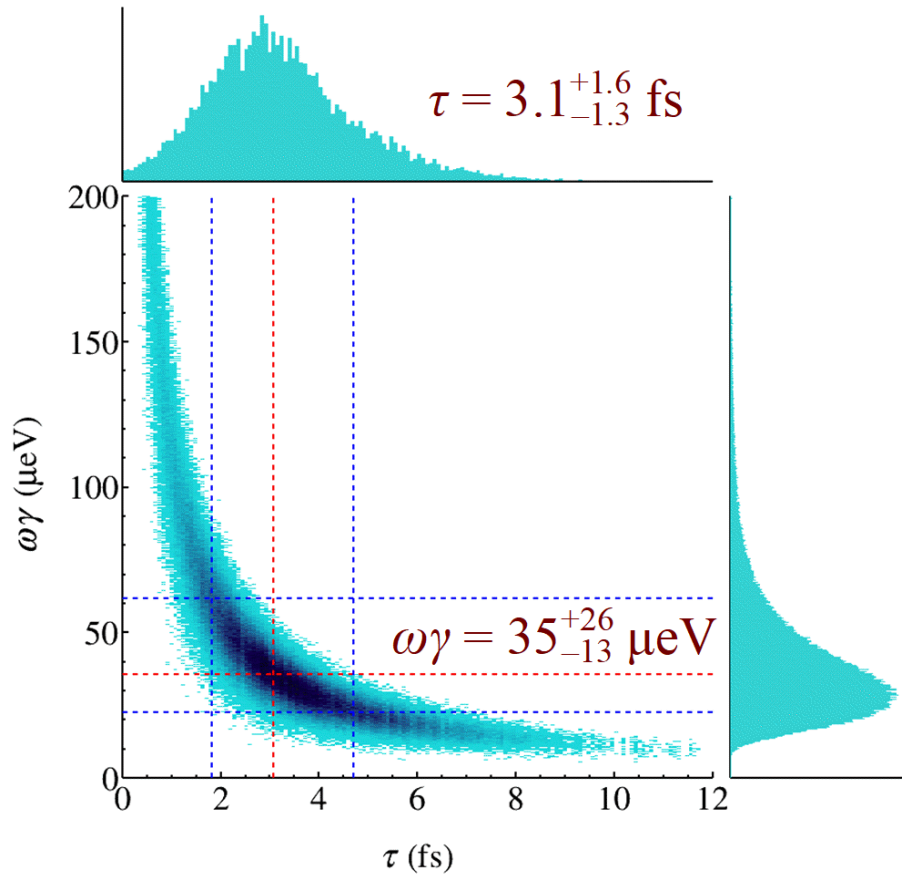
25000 counts

$$\tau = 3.0^{+0.8}_{-0.5} \text{ fs}$$

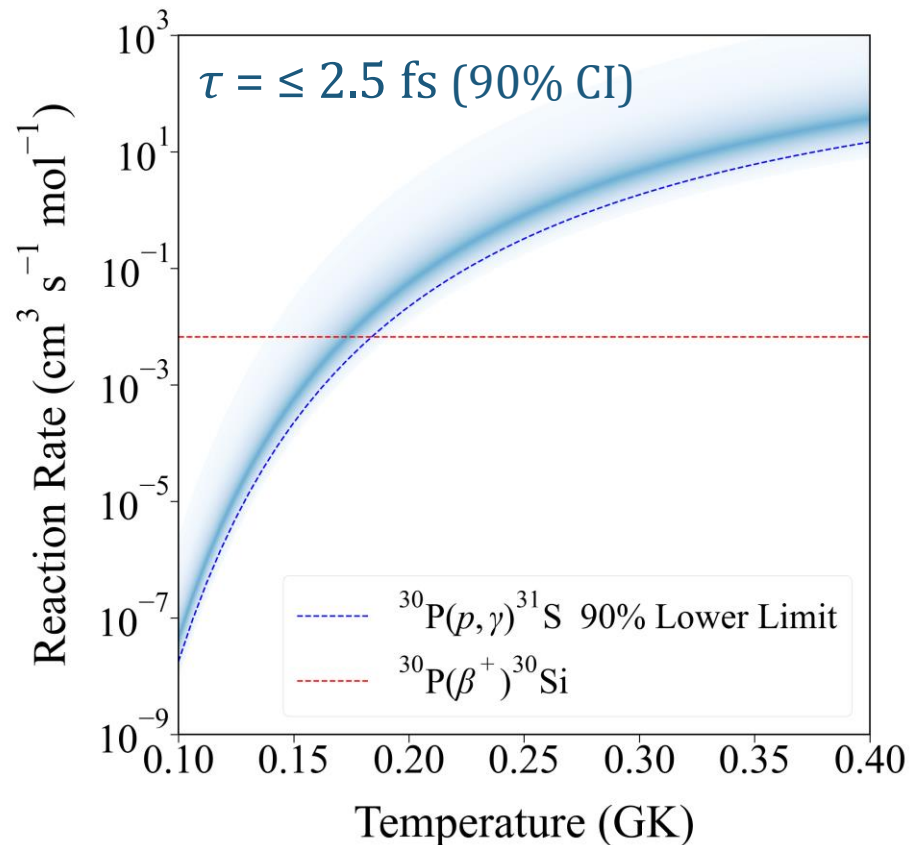
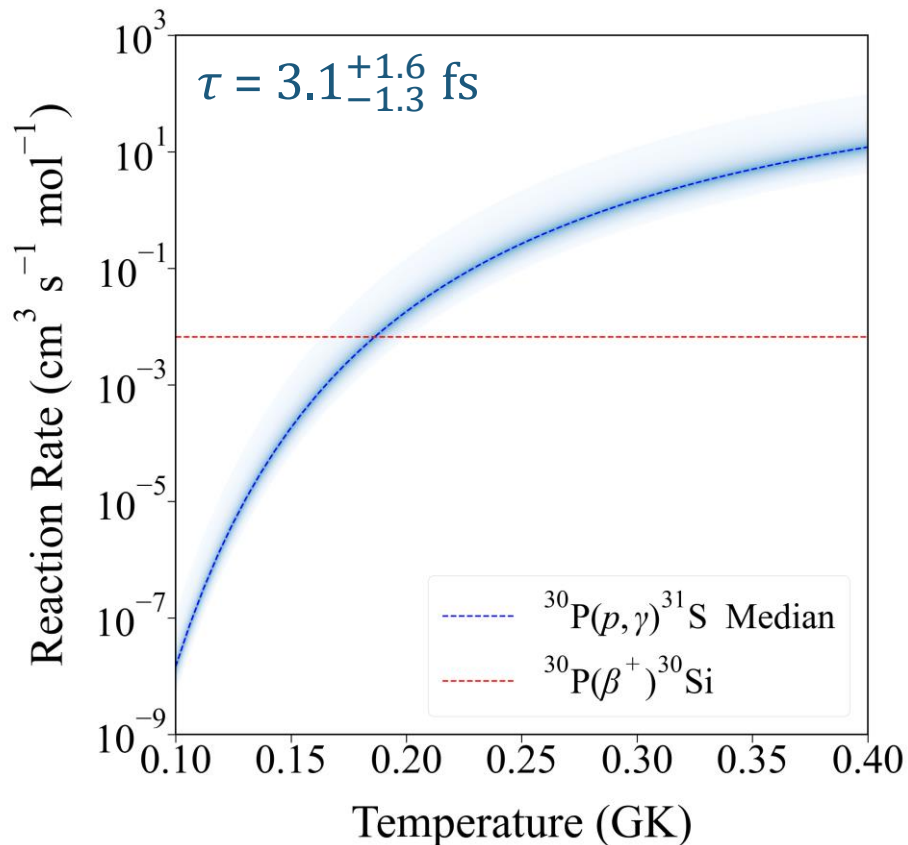
 Prior
 Posterior



Resonance Strength



$^{30}\text{P}(p,\gamma)^{31}\text{S}$ Reaction Rate



Monte Carlo reaction rate calculation <https://github.com/rlongland/RatesMC>

Nova nucleosynthesis model calculation by Jordi José.

Summary

- Our simulation has demonstrated that with 19 shifts, we can either obtain a finite value as low as 3 fs or set a strong upper limit of 2.5 fs on the lifetime of the astrophysically important $3/2^+$, 260-keV $^{30}\text{P}(p,\gamma)^{31}\text{S}$ resonance.
- This level of precision will put the $^{30}\text{P}(p,\gamma)^{31}\text{S}$ reaction rate on a fully experimental footing for the first time, and will potentially eliminate the largest nuclear uncertainty associated with a series of isotopic and elemental abundance ratios in nova ejecta.
 - The new rate will provide valuable insights into identifying the origin of several presolar grains using the $^{29}\text{Si}:^{28}\text{Si}$ and $^{30}\text{Si}:^{28}\text{Si}$ ratios.
 - The new rate will calibrate nova thermometers based on the elemental abundance ratios of **O:S**, **O:P**, **S:Al**, and **P:Al**.
 - The new rate will make the **Si/H** abundance ratio a more accurate constraint on the degree of mixing between the white dwarf's outer layers and the accreted envelope.

Collaboration

B. Davids

TRIUMF/SFU

L. J. Sun

MSU/FRIB

C. Wrede

MSU/FRIB

A. Adams

MSU/FRIB

C. Angus

University of York

A. Banerjee

SINP

T. Budner

ANL

M.Y.H. Chan

Northwestern U.

J. Chen

MSU/FRIB

J. Dopfer

MSU/FRIB

N. Esker

SJSU

M. Friedman

HUJI

C. Fry

LANL

A.B. Garnsworthy

TRIUMF

G. Hackman

TRIUMF

K. Hudson

SFU

J. Jose

UPC

V. Karayonchev

O.S. Kirsebom

L. Le

R. Mahajan

M. Oliver

C. Ruiz

R. Russell

J. Surbrook

Ö. Sürer

V. Vedia

L. Wagner

L. Weghorn

T. Wheeler

J. Wilkinson

E.J. Williams

D. Yates

TRIUMF

Dalhousie U.

SJSU

LSU/FSU

SJSU

TRIUMF

University of Surrey

LANL

Miami U.

TRIUMF

TRIUMF

MSU/FRIB

MSU/FRIB

LLNL

TRIUMF

UBC



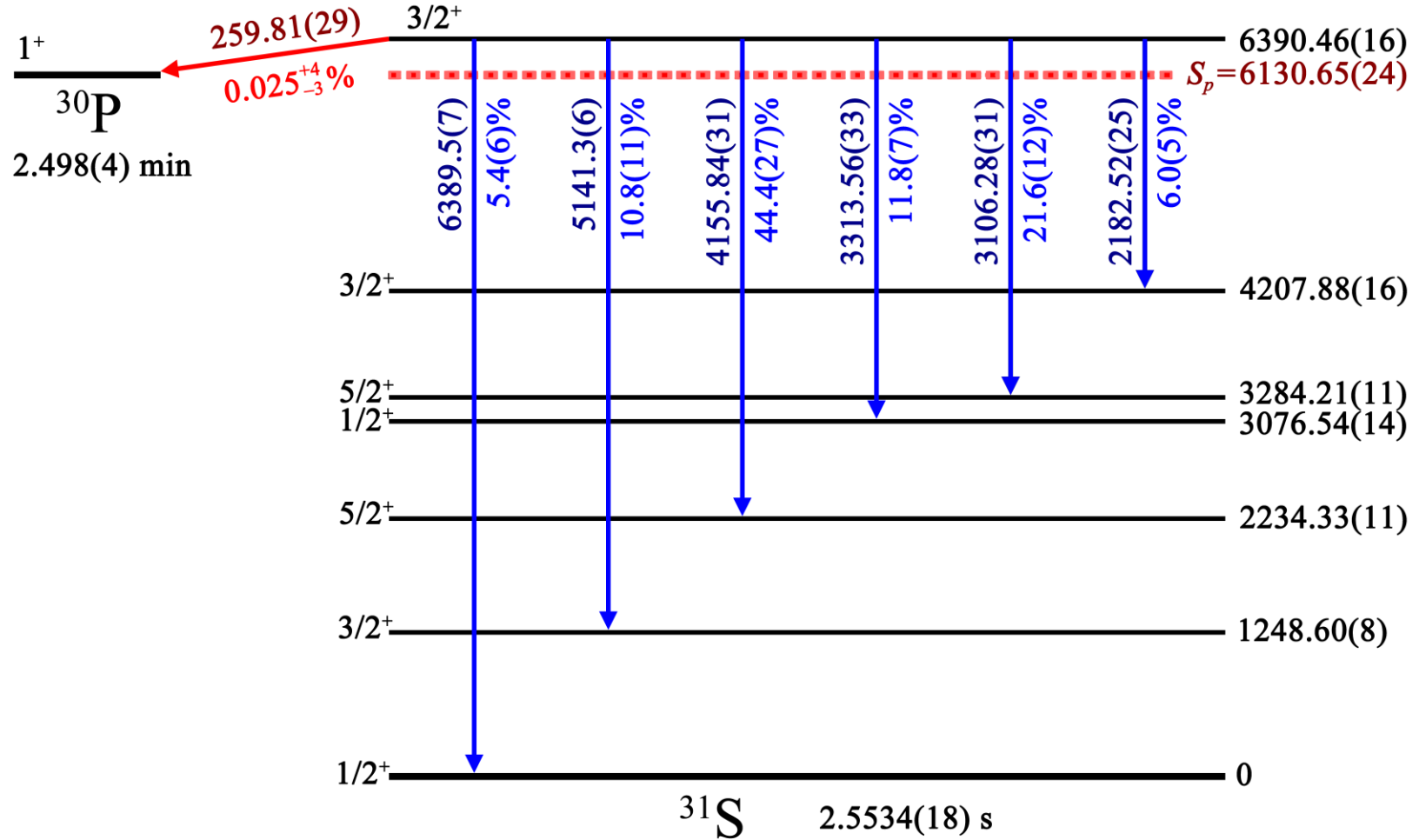
Google - Noto Color Emoji 15.0 (Animated)



Known Lifetimes of ^{31}S Excited States

^{31}S state		Evaluated τ (fs)	Literature
$3/2^+$	1248	720(90)	Engmann NPA 1971 Doornenbal NIMA 2010 Tonev PLB 2021 Herlitzius Thesis 2013 Sun PLB 2023
$5/2^+$	2234	290(80)	Engmann NPA 1971 Sun PLB 2023
$1/2^+$	3076	<11	Sun PLB 2023
$3/2^+$	3435	<16	Sun PLB 2023
$7/2^-$	4450	790(250)	Pattabiraman PRC 2008 Tonev PLB 2021
$(3/2)^-$	4971	<7	Sun PLB 2023
$1/2^+$	5156	<15	Sun PLB 2023
$9/2^-$	6376	245(45)	Pattabiraman PRC 2008
$11/2^{(-)}$	6833	180(35)	Pattabiraman PRC 2008

Known Decay Scheme of the Key Resonance



J. Chen *et al.*, Nucl. Data Sheets 184, 29 (2022).



γ -ray measurements of ^{31}S states around 6.39 MeV

E_x (keV)	J_i^π	E_γ (keV)	E_f (keV)	J_f^π	Reaction / Decay	Reference
6393.7(5)	11/2 ⁺	1090.7(10)	5301	9/2 ⁺	$^{12}\text{C}(^{20}\text{Ne},n)^{31}\text{S}$	Jenkins
		3042.4(4)	3351	7/2 ⁺		
6394.2(2)	11/2 ⁺	1091.2(4)	5301.7(3)	9/2 ⁺	$^{28}\text{Si}(^4\text{He},n)^{31}\text{S}$	Doherty
		3042.9(1)	3351.3(2)	7/2 ⁺		
6393	11/2 ⁺	1090.5(7)	5301	9/2 ⁺	$^{24}\text{Mg}(^{12}\text{C},an)^{31}\text{S}$	Testov
		3042.2(10)	3351	7/2 ⁺		
6392.5(2)	5/2 ⁺	5143.1(2)	1248.5(1)	3/2 ⁺	$^{28}\text{Si}(^4\text{He},n)^{31}\text{S}$	Doherty
6392.5(2)	5/2 ⁺	5145(3)	1248	3/2 ⁺	$^2\text{H}(^{30}\text{P},n)^{31}\text{S}$	Kankainen
6390.2(7)	3/2 ⁺	2182.52(25)	4207.7(31)	3/2 ⁺	$^{31}\text{Cl}(\beta^+\gamma)^{31}\text{S}$	Bennett
		3106.28(31)	3283.76(31)	5/2 ⁺		
		3313.56(33)	3076.40(31)	1/2 ⁺		
		4155.84(31)	2234.06(20)	5/2 ⁺		
		5141.3(6)	1248.43(20)	3/2 ⁺		
		6389.5(7)	0	1/2 ⁺		

³He Implanted Target

SRIM-2013.00
File Help, FAQ and Scientific Explanations

ION
Ion Type He 3 amu
Ion Energy 30 keV
Ion Angle 0 degrees
Completed 120000 of 120000
SHOW LIVE DATA HELP

TARGET DATA
? He (30) into Layer 1 (1 layers, 1 atoms)

Layer Name	Width (A)	Density	Au (196.9)	Solid/Gas	Stop Corr.
1 Layer 1	3000	19.311	1.00000	Solid	1

Lattice Binding Energy 3
Surface Binding Energy 3.8
Displacement Energy 25

Calculation Parameters
Backscattered Ions 18739
Transmitted Ions 0
Vacancies/Ion 27.4

ION STATS
Range Straggle
Longitudinal 800 A 393 A
Lateral Proj. 434 A 535 A
Radial 681 A 329 A

Type of Damage Calculation
Quick: Kinchin-Pease
Stopping Power Version
SRIM-2008

% ENERGY LOSS
Ions Recoils
Ionization 90.84 0.74
Vacancies 0.17 0.12
Phonons 1.61 6.52

SPUTTERING YIELD
Atoms/ion eV/Atom
TOTAL
Au 0.000000 0.00

Save every 10000 ions
Random Number 44709391
Counter HELP

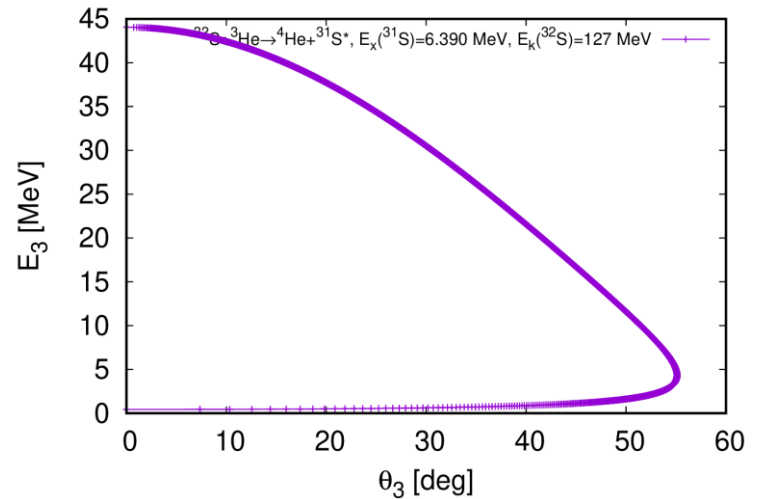
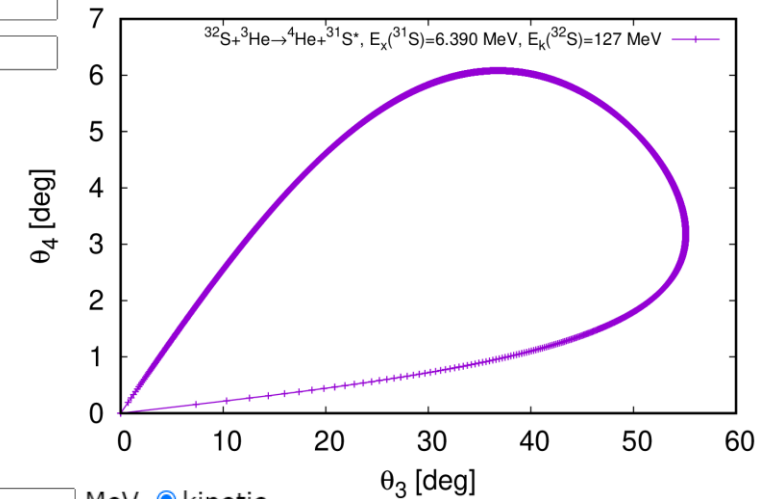
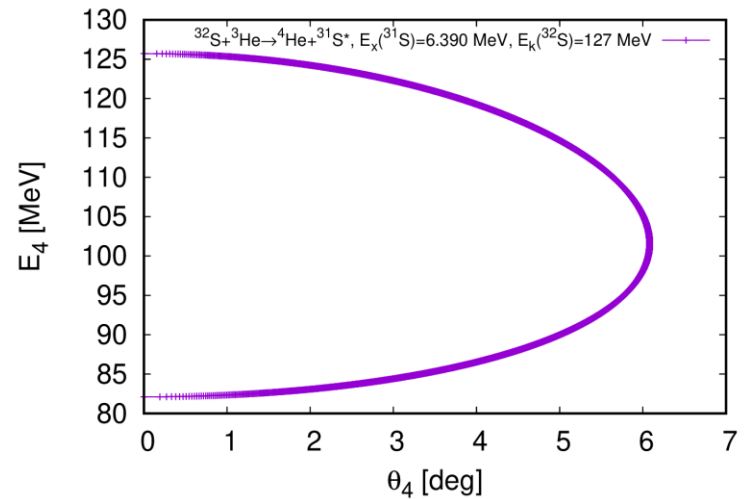
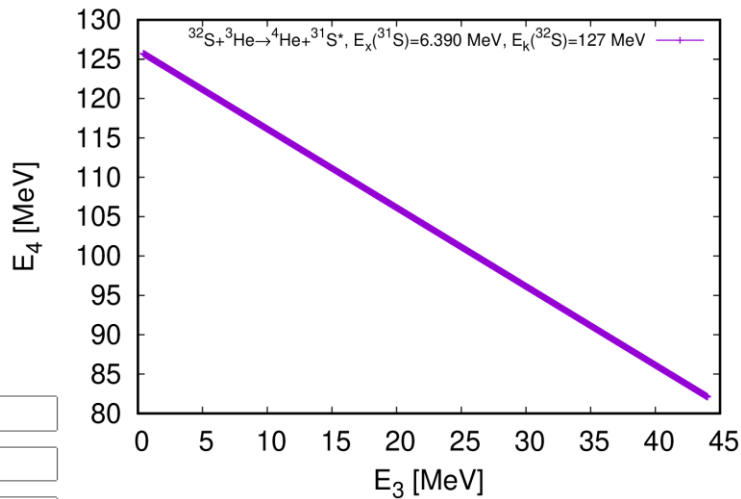
ION RANGE Distribution
ION RANGES
Ion Range = 800 A Skewness = 0.2674
Straggle = 393 A Kurtosis = 2.5670

File Plot DISTRIBUTIONS
Ion Distribution
Ion/Recoil Distribution
Lateral Range
Ionization
Phonons
Energy to Recoils
Damage Events
Integral Sputtered
Differential Ions
Backscattered Ions
Transmitted Ions
Collision Details
3-D Plots 3D Help
Ion Distribution 3D
Recoil-Dist. 3D
Ionization 3D
Phonons 3D
Target Damage 3D

Save Save As Print Help



Reaction Kinematics



Projectile (m_1):

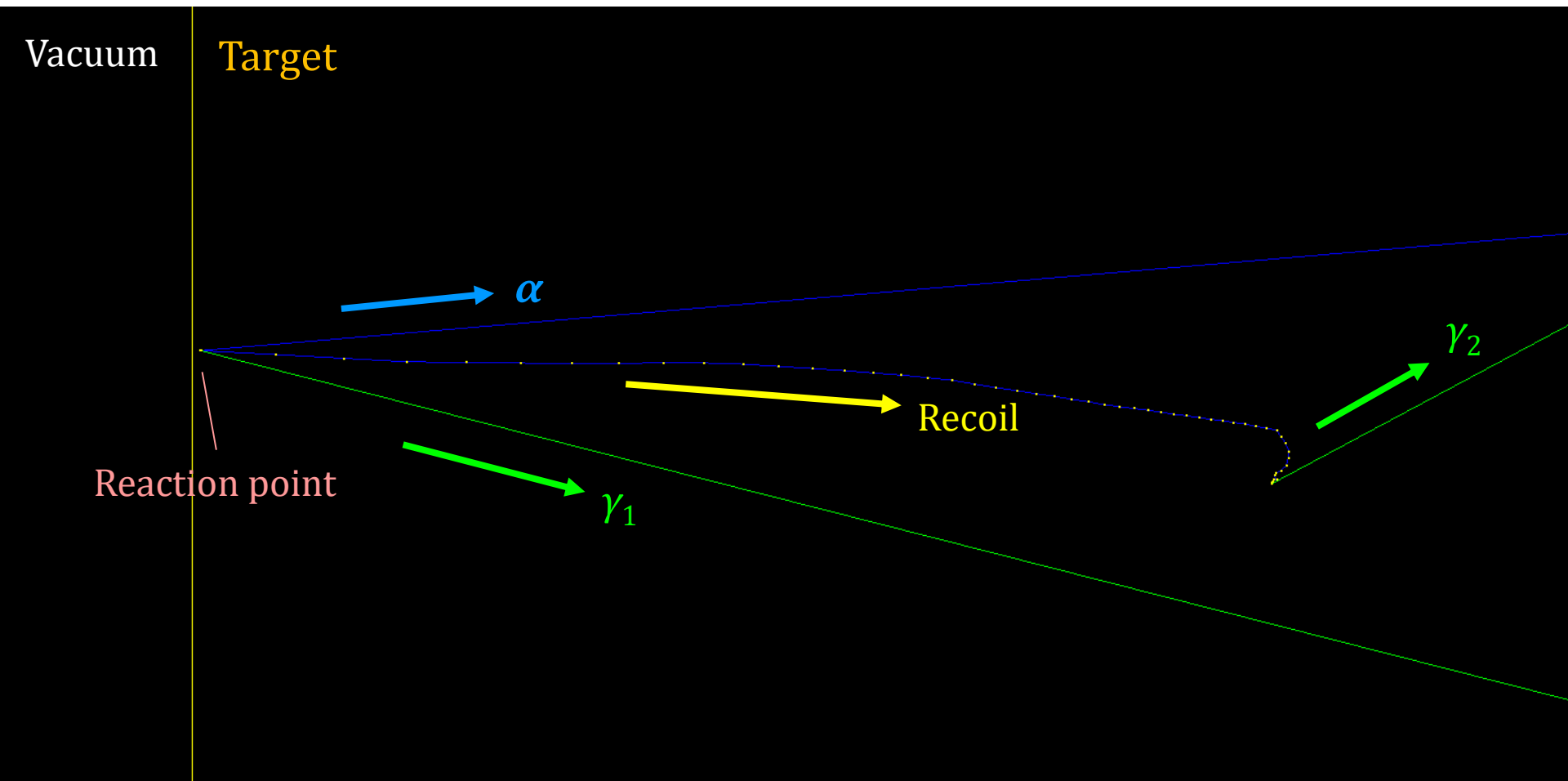
Target (m_2):

Ejectile (m_3):

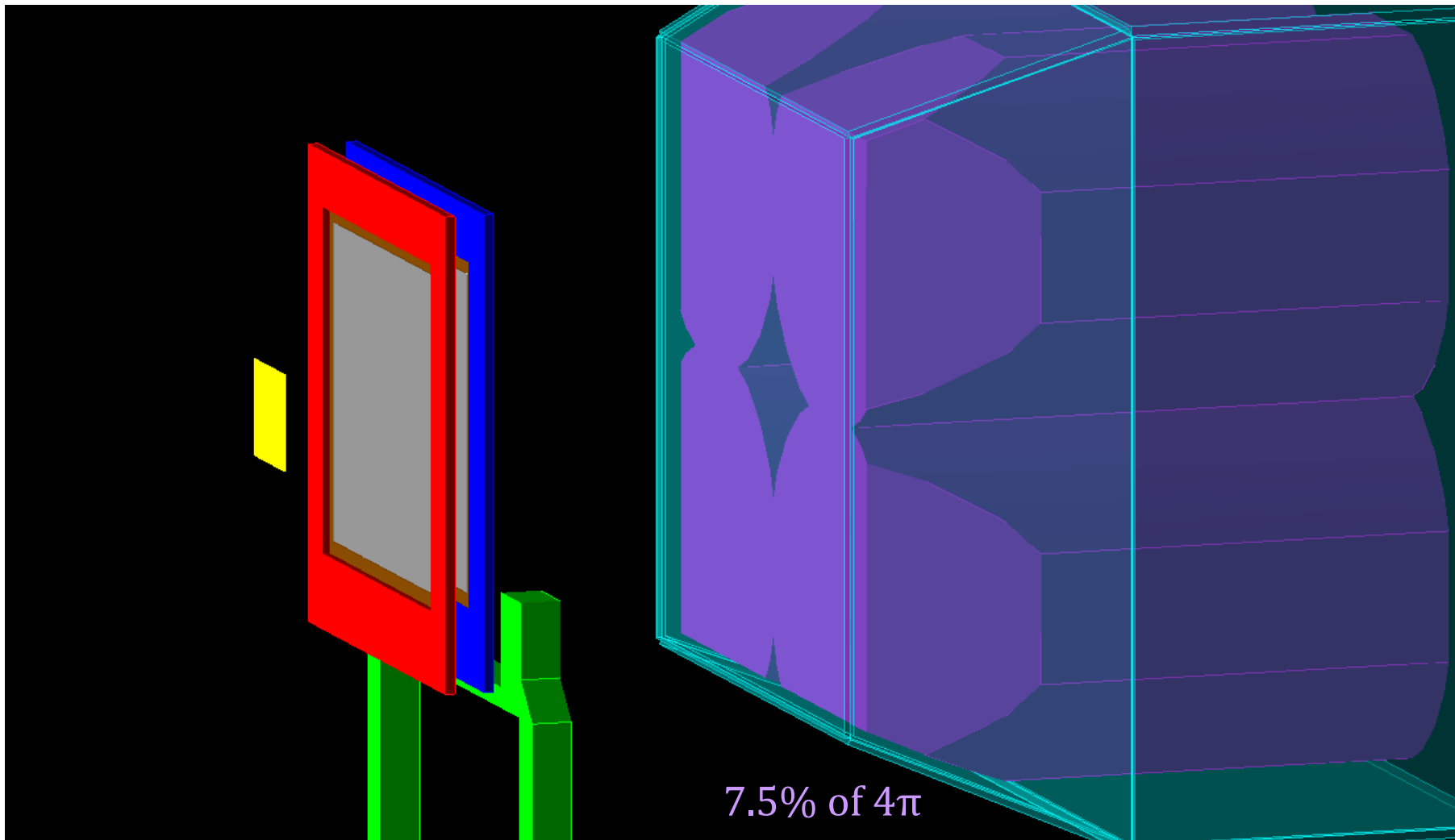
Recoil (m_4):

Projectile Energy: MeV kinetic

Geant4 Simulation



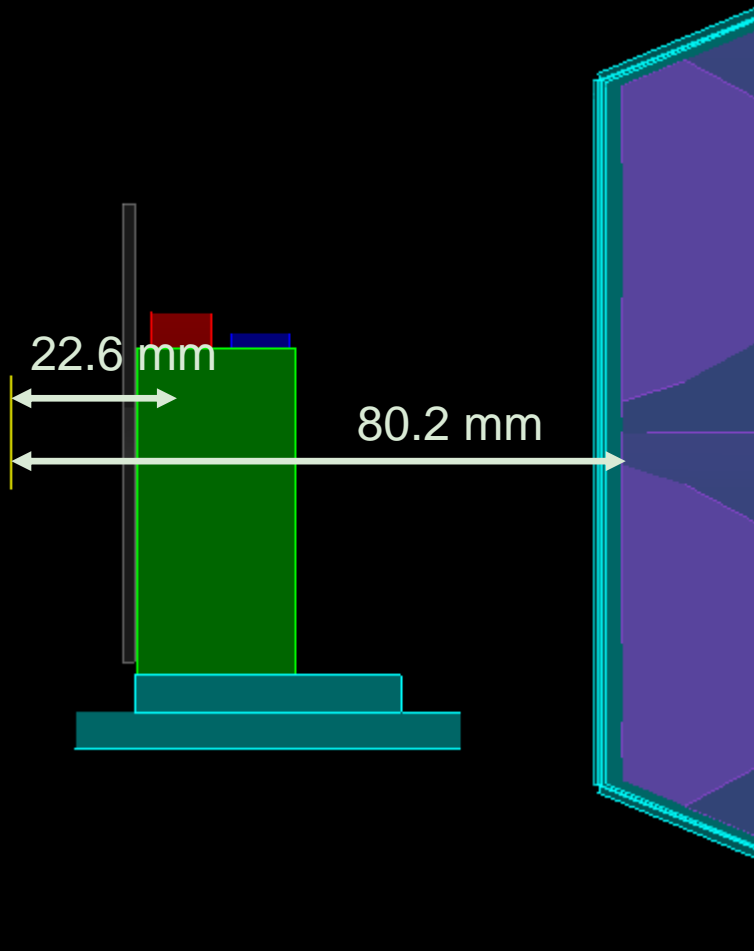
Geant4 Simulation



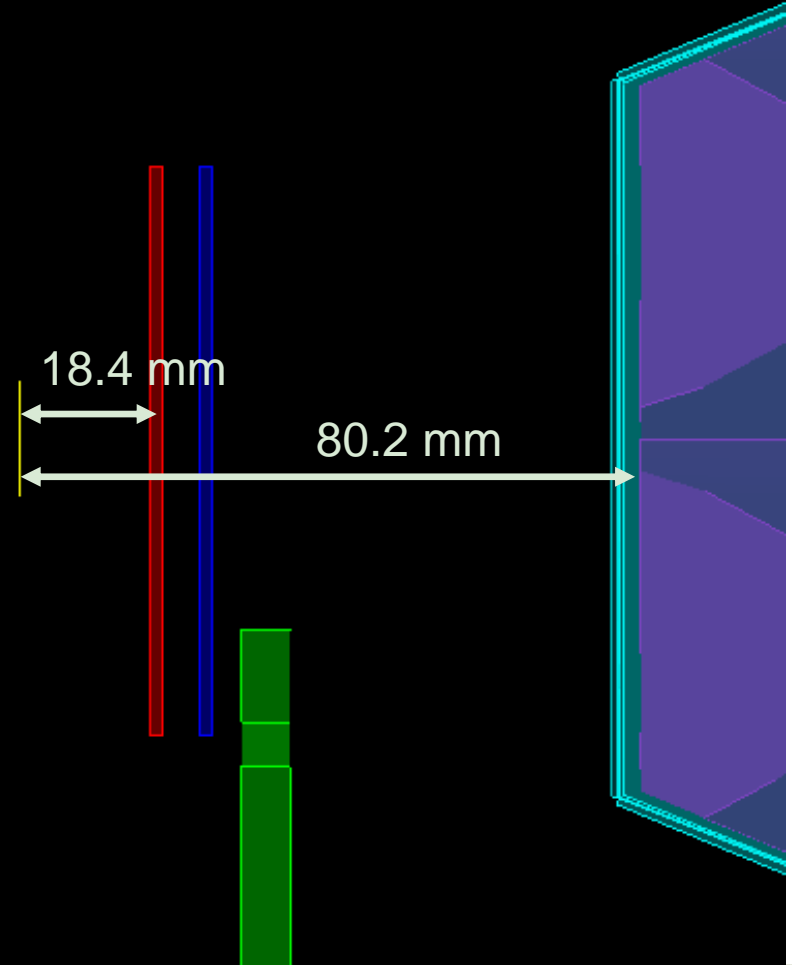
7.5% of 4π

Solid Angle

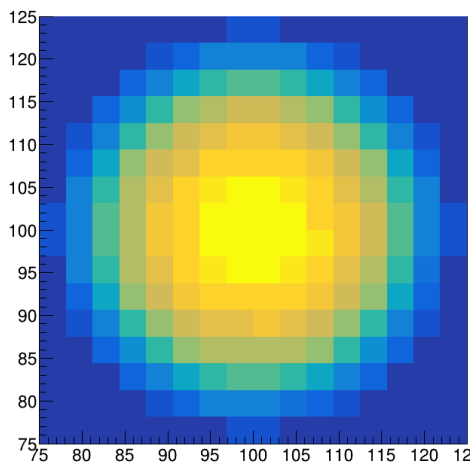
DSL1



DSL2

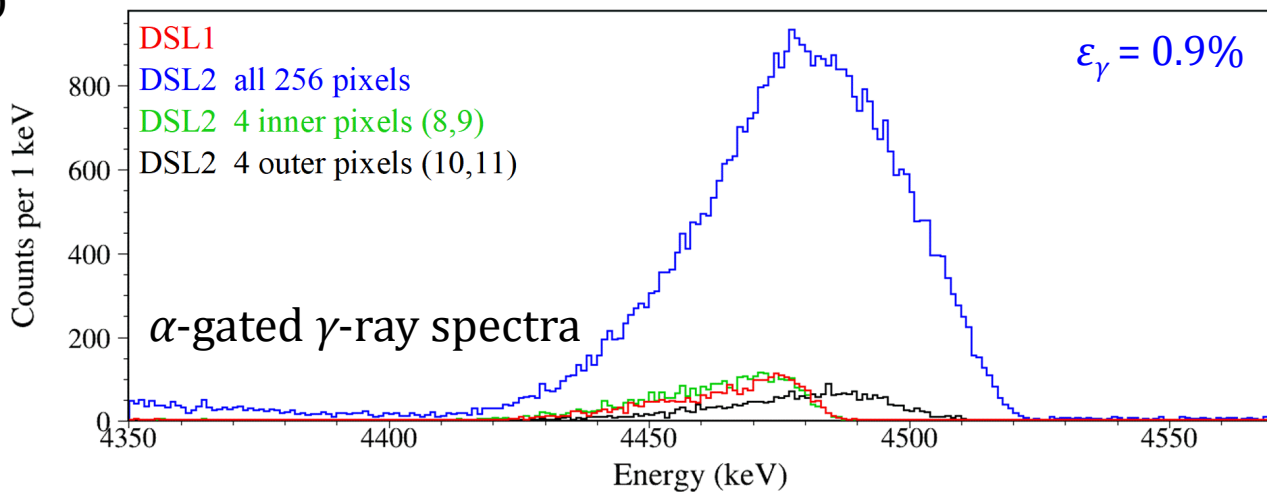
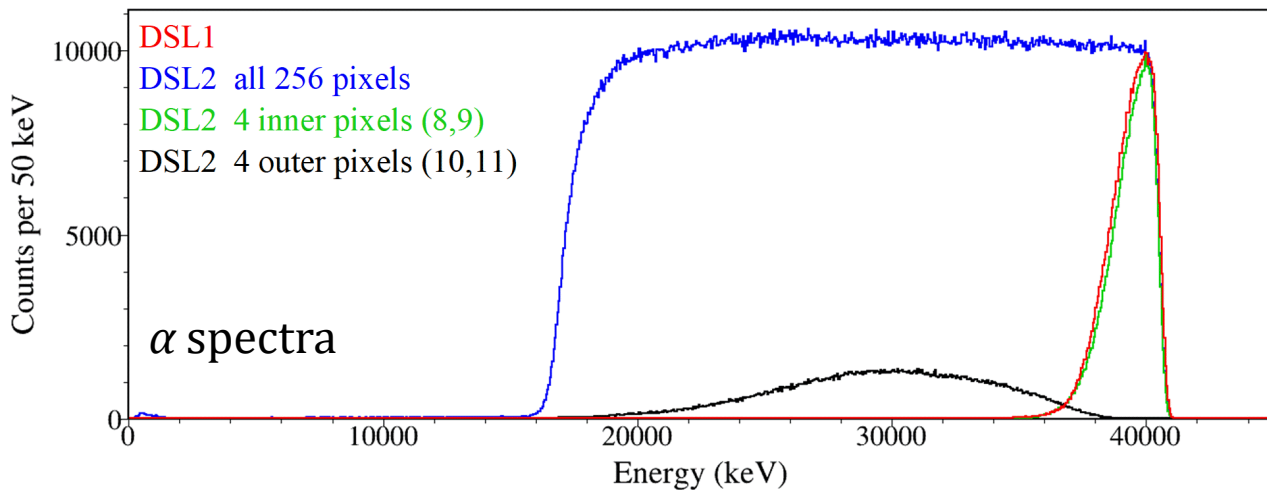


Geant4 Simulation

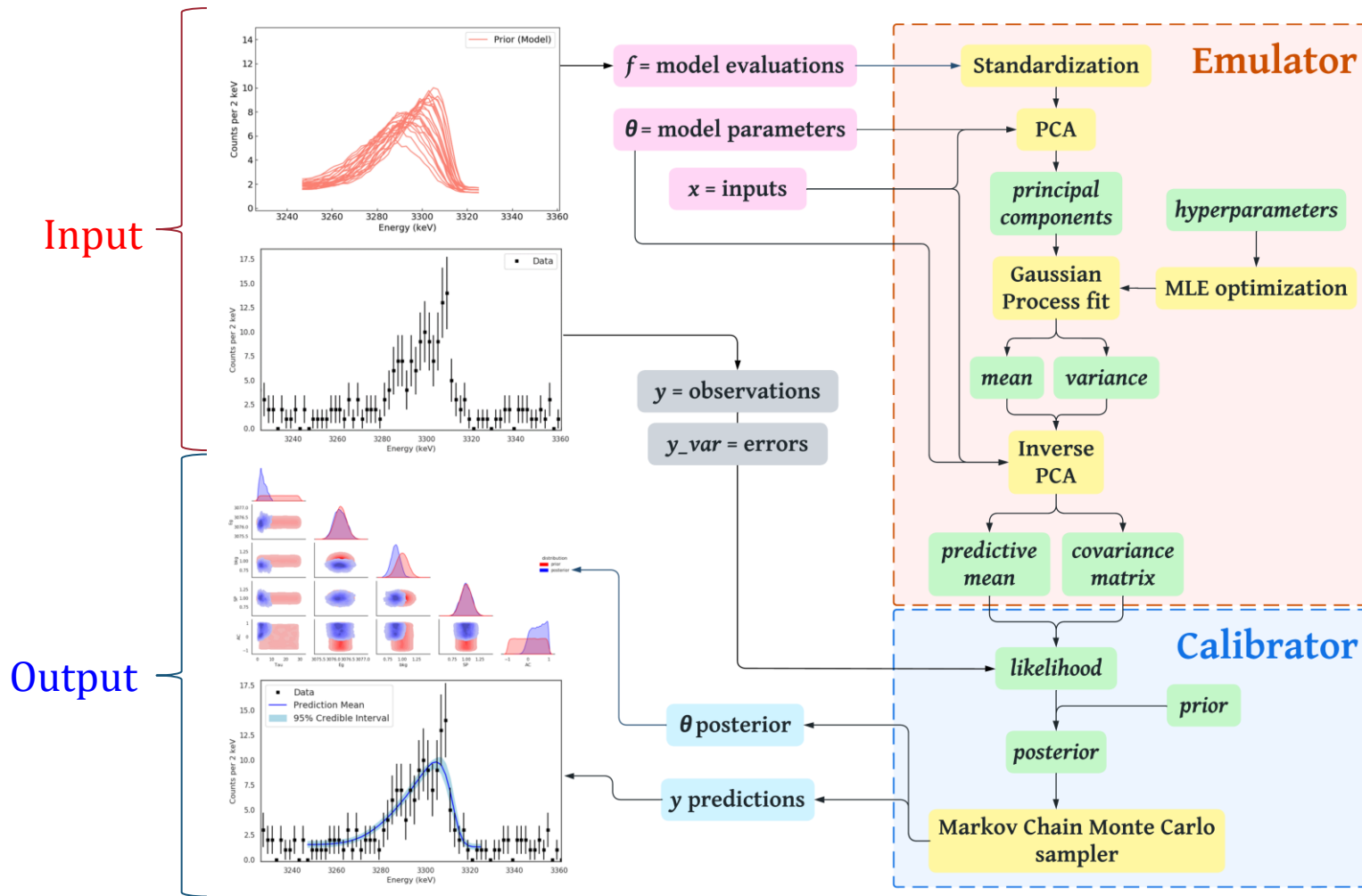


α particle heatmap on DSSD

1 pixel: 0.21% of 4π

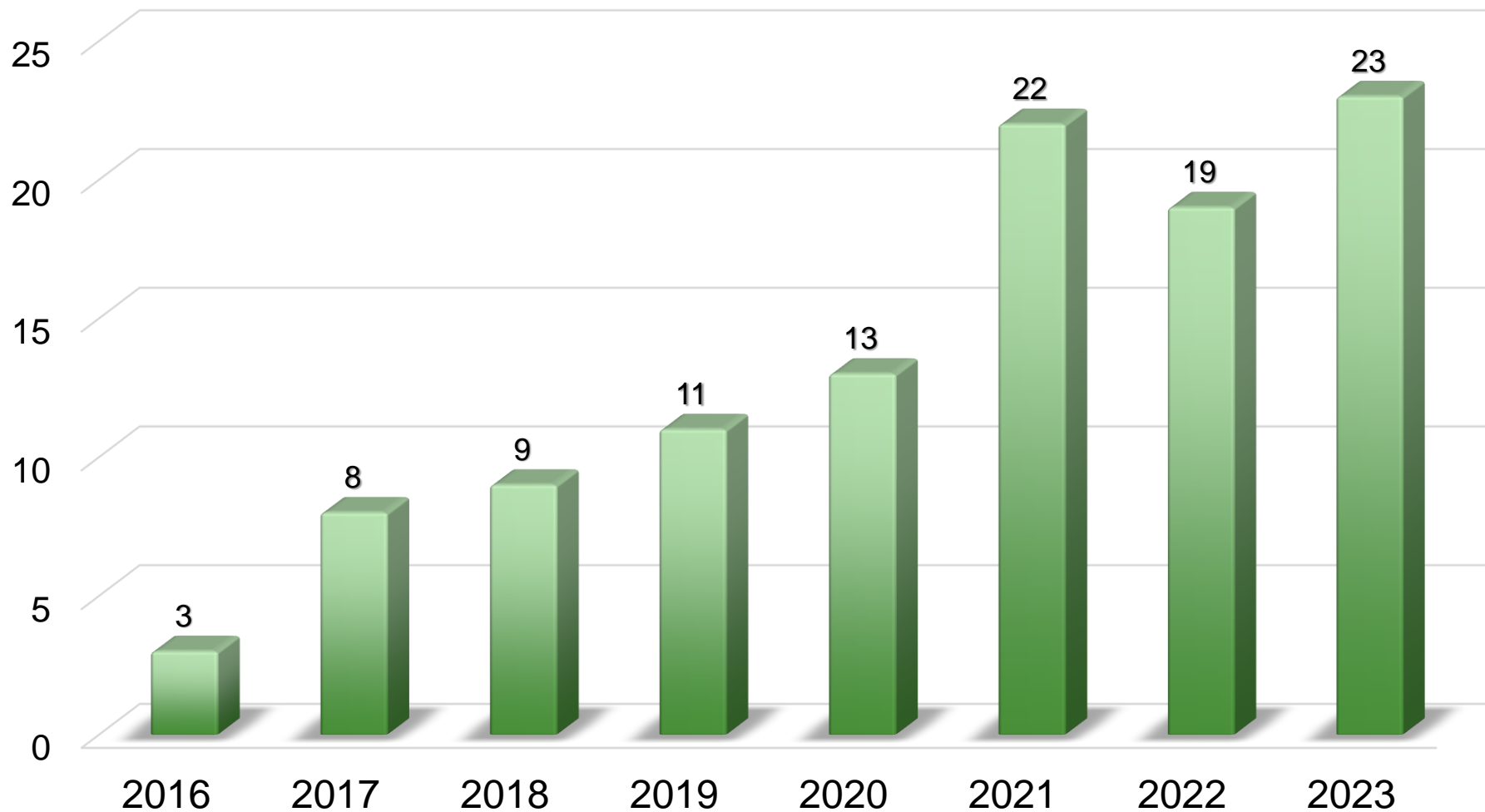


Bayesian Model Emulation & Model Calibration



Ö. Sürer *et al.*, Phys. Rev. C 106, 024607 (2022).

Bayesian-related talks at each APS DNP Meeting



Advantages of Inverse Kinematics

While DSAM can in principle be done in either normal or inverse kinematics, there are several advantages to inverse kinematics, where a heavy beam impinges on a light target, including:

- Recoils tend to be in the electronic stopping power regime. Electronic stopping powers are both more easily measured and have smaller angular scattering, leading to smaller uncertainties in the extracted lifetimes.
- Velocity change can be larger, due to a maximum in stopping powers for typical systems around recoil energies of tens of MeV for nuclei with mass number $20 < A < 40$. This is particularly helpful for extracting finite lifetimes for short-lived states.
- Higher recoil velocities ($\beta = 0.074$) lead to larger Doppler shifts, making it easier to distinguish unshifted peaks from shifted peaks, particularly at low energies, where the absolute shift is small.

C. Fry, Ph.D. Thesis, Michigan State University, USA, 2018.



Readiness

S2373 **Lifetime of the key $^{30}\text{P}(p,\gamma)^{31}\text{S}$ resonance in novae (DSL)**

Spokespersons: B. Davids, L.J. Sun, C. Wrede

Isotope	Minimum Intensity (s-1)	Requested Intensity (s-1)	Target & Ion Source	Energy	Comment
^{32}S	0.6E+10	1.8E+10	OLIS	128 MeV	

Comments: ^{32}S 7+ was already delivered to DSL in Aug 2018 at 1E+11 pps, with acceptable contaminant levels. Thus this is feasible. However the new OLIS team (C. Charles) has not yet had experience of producing this beam so some practice time with OLIS should be taken into account well in advance of experiment.

Classification for Beam Delivery or Development

Proposals or Progress Reports:

feasible

marginal

infeasible

Letters of Intent:

trivial

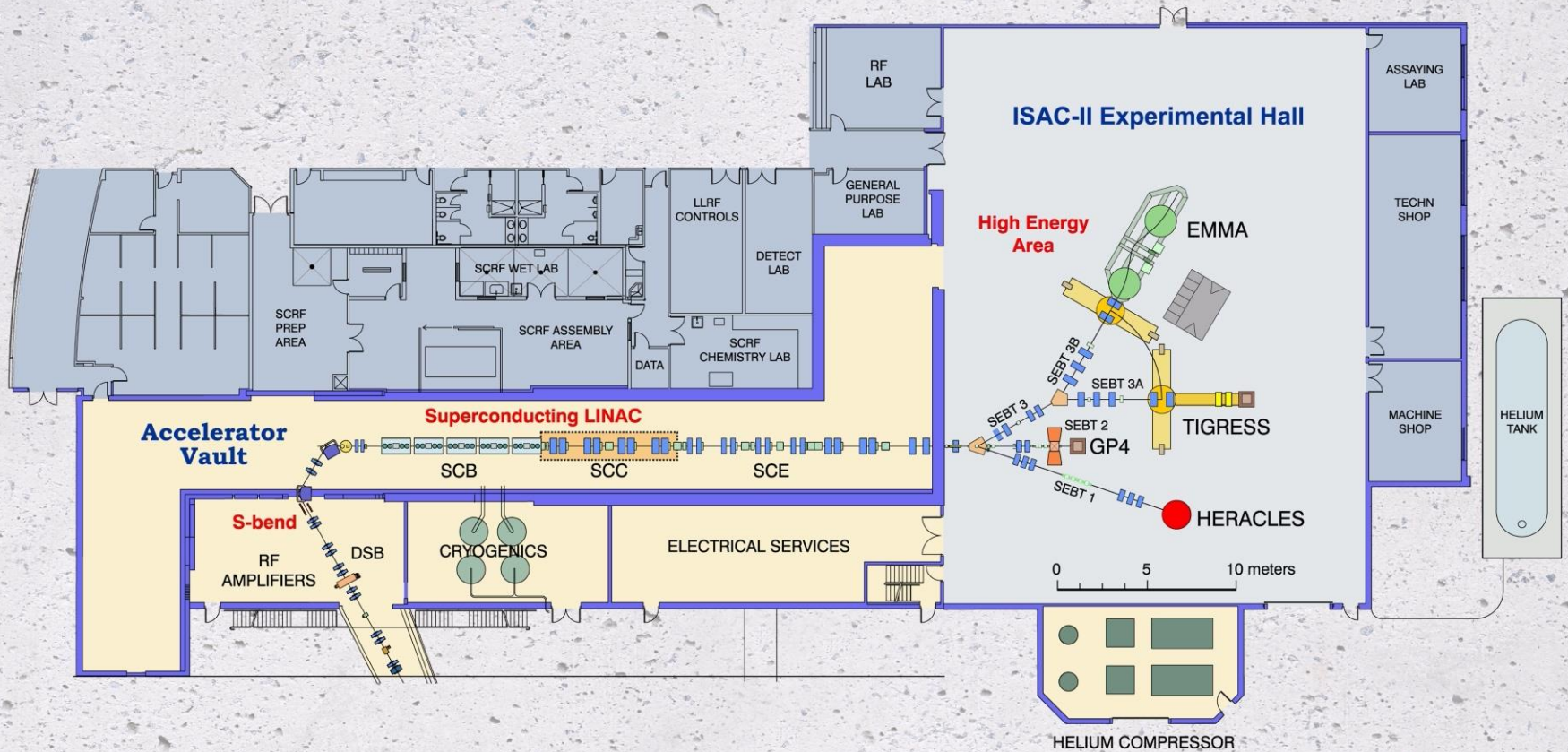
complex

major

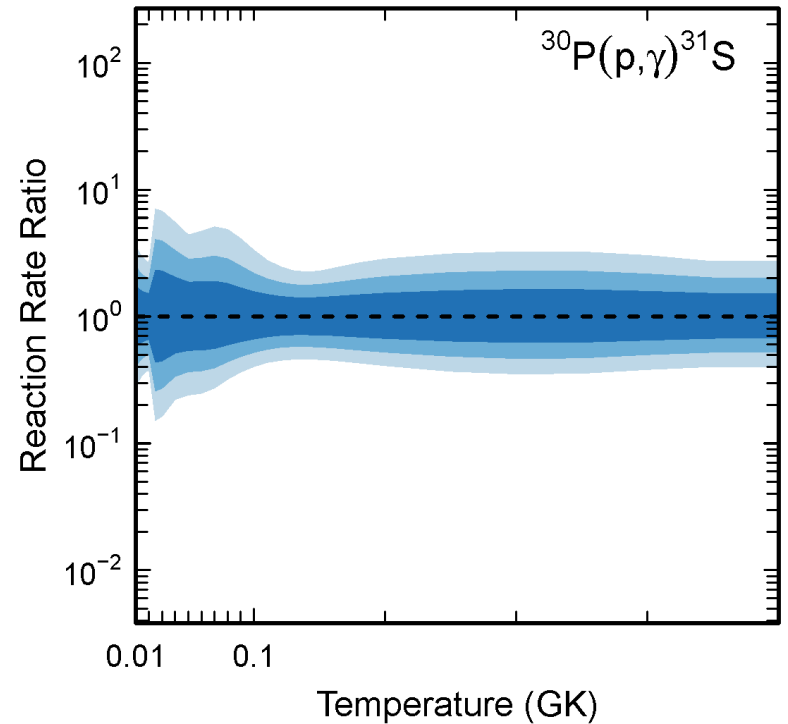
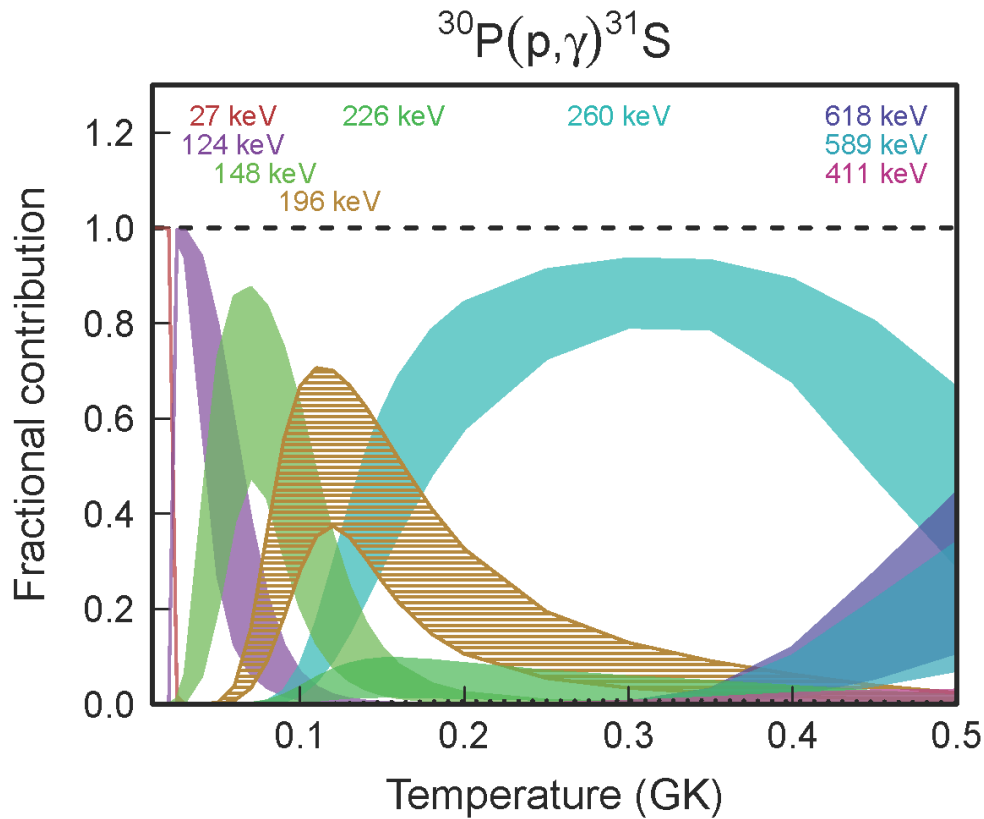
We possess all the equipment and targets needed for the experiment at TRIUMF.

Beam Delivery

ISAC-II Experimental Hall



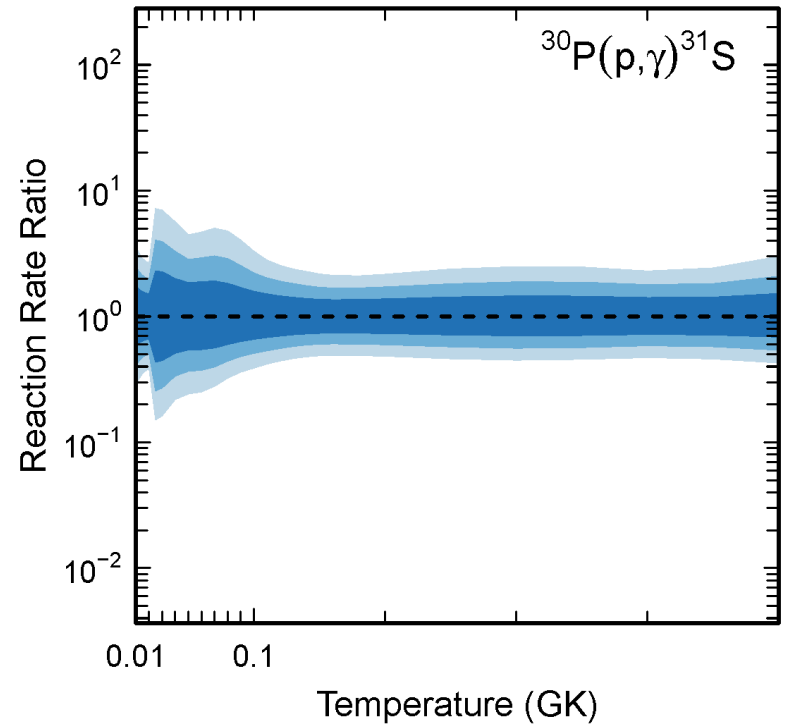
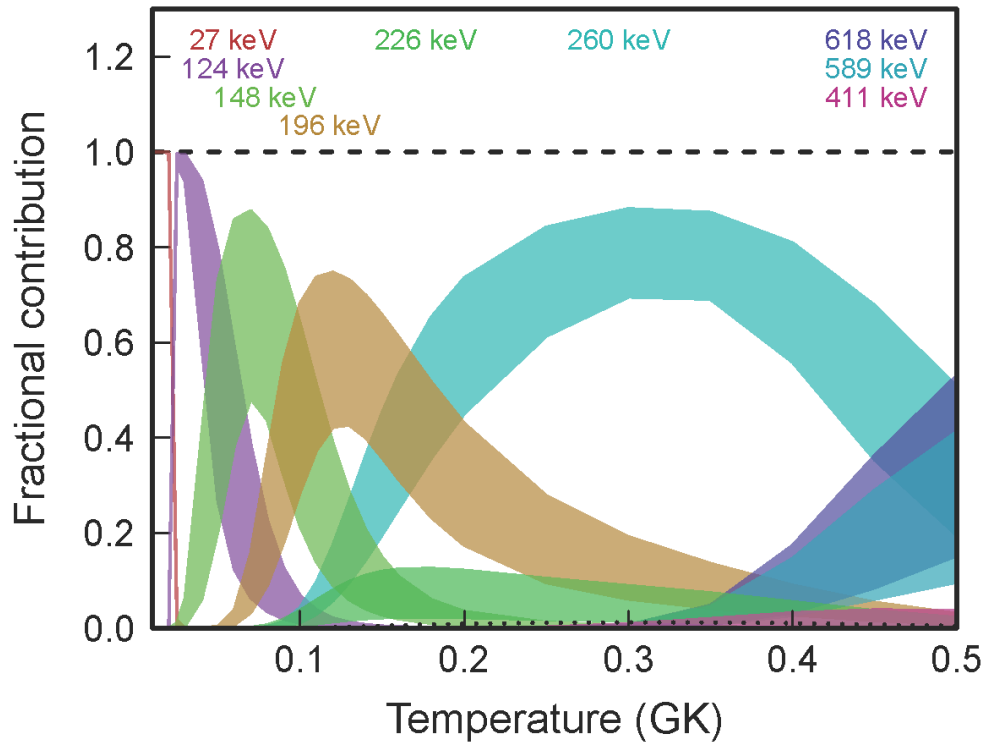
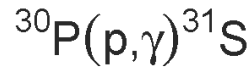
RatesMC



$$\omega\gamma_{260} = 80(48) \mu\text{eV}$$

T. Budner *et al.*, Phys. Rev. Lett. 128, 182701 (2022).

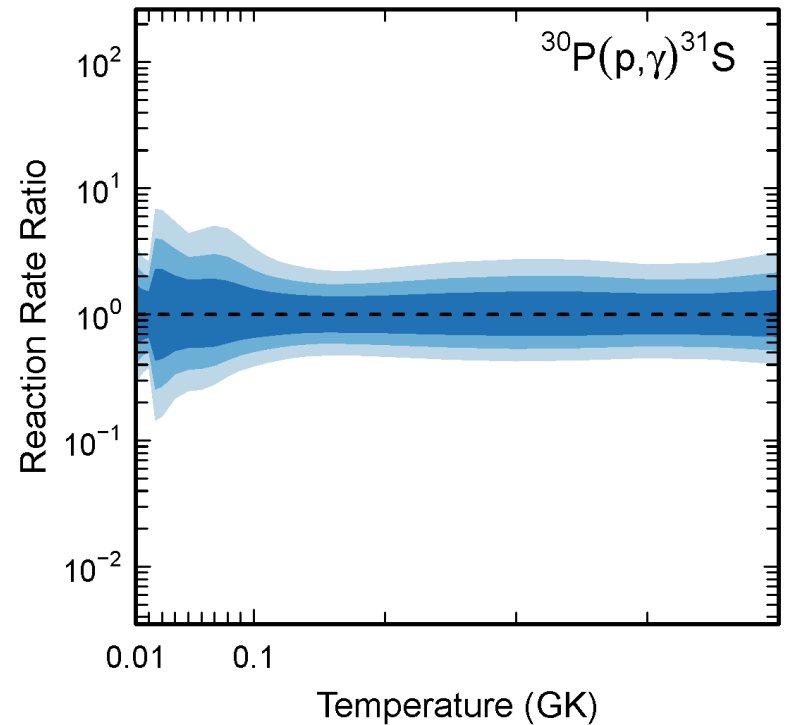
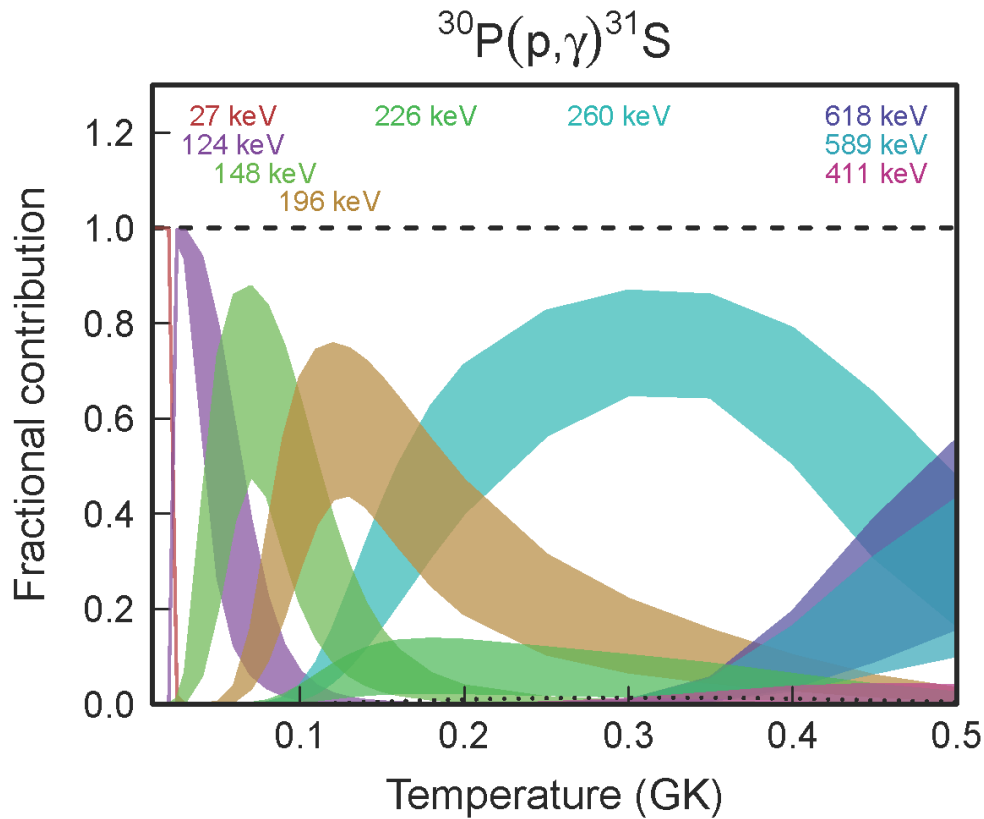
RatesMC



$$\omega\gamma_{260} = 22 - 62 \mu\text{eV} \quad 1000 \text{ counts} \quad \tau = 3 \text{ fs}$$



RatesMC



$$\omega\gamma_{260} = 18 - 57 \mu\text{eV} \quad 500 \text{ counts} \quad \tau = 3 \text{ fs}$$

RatesMC

```
*****
Resonant Contribution
Note: G1 = entrance channel, G2 = exit channel, G3 = spectator channel !! Ecm, Exf in (keV); wg, Gx in (eV) !
Note: if Er<0, theta^2=C2S*theta_sp^2 must be entered instead of entrance channel partial width
Ecm  DEcm  wg    Dwg   J   G1    DG1    L1  G2    DG2    L2  G3  DG3  L3  Exf  Int  Corr/Frac
 27.05 0.38 1.1e-33 0.4e-33 3.5 0 0 0 0 0 0 0 0 0 0.0 0
124.45 0.38 9.5e-12 9.5e-12 0.5 0 0 0 0 0 0 0 0 0 0.0 0
148.45 0.27 2.1e-9 2.1e-9 1.5 0 0 0 0 0 0 0 0 0 0.0 0
196.15 0.55 5.1e-7 2.7e-7 1.5 0 0 0 0 0 0 0 0 0 0.0 0
226.41 0.33 0.7e-6 0.7e-6 2.5 0 0 0 0 0 0 0 0 0 0.0 0
244.95 0.38 6.1e-8 2.1e-8 4.5 0 0 0 0 0 0 0 0 0 0.0 0
259.81 0.29 8.0e-5 4.8e-5 1.5 0 0 0 0 0 0 0 0 0 0.0 0
261.51 0.33 5.8e-7 2.5e-7 2.5 0 0 0 0 0 0 0 0 0 0.0 0
262.28 0.31 1.0e-30 1.0e-30 5.5 0 0 0 0 0 0 0 0 0 0.0 0
271.35 2.01 1.0e-30 1.0e-30 3.5 0 0 0 0 0 0 0 0 0 0.0 0
410.95 0.47 0.85e-4 0.85e-4 1.5 0 0 0 0 0 0 0 0 0 0.0 0
451.75 2.01 1.0e-30 1.0e-30 3.5 0 0 0 0 0 0 0 0 0 0.0 0
503.99 0.33 1.0e-30 1.0e-30 4.5 0 0 0 0 0 0 0 0 0 0.0 0
589.35 1.03 0.072 0.072 2.5 0 0 0 0 0 0 0 0 0 0.0 0
618.35 2.01 0.200 0.200 1.5 0 0 0 0 0 0 0 0 0 0.0 0
*****
```

$$\omega\gamma = 80(48) \mu\text{eV}$$

